

E- 6735

N 72 - 15990

**NASA TECHNICAL
MEMORANDUM**

NASA TM X- 67989

NASA TM X- 67989

**CASE FILE
COPY**

**PRELIMINARY PERFORMANCE OF THE BRAYTON 4 25-INCH RADIAL
COMPRESSOR OPERATING IN A HELIUM-XENON GAS MIXTURE**

by Armen Asadourian, Thomas P. Hecker, and Roman Kruchowy
Lewis Research Center
Cleveland, Ohio
December, 1971

This information is being published in preliminary form
in order to expedite its early release.

PRELIMINARY PERFORMANCE OF THE BRAYTON 4.25-INCH RADIAL
COMPRESSOR OPERATING IN A HELIUM-XENON GAS MIXTURE

by

Armen Asadourian, Thomas P. Hecker, and Roman Kruchowy

Lewis Research Center

SUMMARY

The performance of a 4.25-inch radial compressor was evaluated using a helium-xenon gas mixture. Compressor performance was mapped during the Brayton cycle power system testing at Lewis Research Center. The range of testing included three shaft speeds: the design speed of 36,000 rpm, 10 percent overspeed (39,600 rpm), and 10 percent underspeed (32,400 rpm). A range of compressor inlet temperatures from 60° F to 120° F and discharge pressures from 20 to 45 psia was included. The effects of turbine inlet temperatures (from 1200° F to 1600° F) on the compressor were also studied. The data presented include plots of weight flow, compressor pressure ratio, efficiency, and temperature-rise ratio.

INTRODUCTION

Several electrical power generating systems have been designed and developed for space applications. A system which has considerable interest is a single-shaft dynamic system which operates on a Brayton thermodynamic cycle. The system is designed to provide 2 to 15 kW of useable power at 1200 Hz.

The power system consists of two major components, viz., a Brayton rotating unit (BRU - a turbine, alternator, and compressor supported on a single shaft by gas bearings) and a set of heat exchangers (ref. 1). The turbomachinery is designed to operate at 36,000 rpm. A helium-xenon gas mixture, which has a molecular weight of nominal 83.8, was used as the working fluid and was heated by an electric heat source. Previous studies of the BRU performance, operating with argon and krypton gas, are reported in reference 2. An investigation of the power system operating with krypton gas is presented in reference 3 while the system

using a helium-xenon gas mixture is evaluated in references 4 and 5. A study of the performance, in argon, of the 4.25-inch compressor which is used in the BRU is evaluated in reference 6.

Preliminary results of an investigation of the performance of the 4.25-inch compressor operating as a component of the power system and with helium-xenon gas are presented in this report. Data are presented for ranges of compressor inlet temperatures, compressor discharge pressures, and speeds. The effects of turbine inlet temperatures from 1200° F to 1600° F on compressor performance were also studied. The data presented herein cover a broad spectrum of compressor operating conditions, using helium-xenon gas, and will be useful in future design work in power systems of this type.

APPARATUS AND PROCEDURE

Description of Compressor

The radial compressor under study was designed for a nominal 6-kilowatt Brayton cycle space electrical power system. The working fluid for the system is a mixture of helium-xenon (He-Xe) gas having a molecular weight of nominal 83.8. A summary of compressor design point values for the reference design power level is given in Table 1. Additional information on the compressor design can be found in references 6 and 7.

The compressor impeller has 15 blades that at the impeller exit are curved backward 30° from radial. The impeller-inlet blade-tip diameter is 2.60 inches. At its exit, the impeller is 4.25 inches in diameter and has a blade height of .205 inch. A vaneless diffuser occupies a .085-inch radial gap between the impeller exit and the vaned diffuser. The vaned diffuser contains 17 vanes .213 inch high that are an integral part of the scroll assembly.

Test Facility

The compressor was tested as part of the overall testing of the Brayton cycle power system at NASA-Lewis Research Center. A schematic diagram of the system is shown in Appendix A.

The system main components are the Brayton rotating unit (BRU) and the Brayton heat exchanger unit (BHXU). The test support equipment includes an electric heat source, a gas-management module, a gas-reclamation module, and a heat-rejection module. The entire gas loop was insulated with a high-temperature quartz blanket. The insulation was generally 6 inches thick; the duct from the waste heat exchanger to the compressor inlet, the compressor itself, and the ducting from the compressor to the recuperator's high-pressure

side inlet were enclosed by 2 inches of insulation. The BRU speed was controlled by a speed control utilizing a parasitic load bank to dissipate generated power in excess of that consumed by a simulated vehicle load. A complete description of the Brayton cycle main components and test support equipment can be found in reference 3.

Instrumentation

Instrumentation used consisted of pressure transducers, temperature sensors, turbine flowmeters, capacitance-type proximity probes, and speed sensors. Absolute pressures were measured by means of a static-pressure tap and a strain-gage type of transducer at both the inlet and outlet of the compressor. For the venturi at the compressor inlet, differential pressure was measured with a differential strain-gage transducer; gas flow rate was calculated accordingly. The BRU bearing clearances were sensed by means of capacitance type of proximity probes.

All data were recorded by means of an on-line digital data system and printed out in engineering units by an electric typewriter.

Procedure

The gas-loop startup and shutdown techniques were similar to those described in reference 3. During the test, constant values of BRU speed, compressor inlet temperature, and turbine inlet temperature were maintained while compressor discharge pressure was varied.

The investigation was conducted through a turbine inlet temperature range of 1200 to 1600^o F and compressor discharge pressure range of 20 to 45 psia at compressor inlet temperatures of 60, 80, 100, and 120^o F. The BRU was also tested at three different speeds: the designed speed of 36,000 rpm, 10 percent over design speed (39,600 rpm), and 10 percent under design speed (32,400 rpm).

The turbine inlet temperature was set by a power controller for the electric heater and was maintained within $\pm 3^{\circ}$ F of the nominal value. Compressor discharge pressure was set by changing the gas inventory in the loop and was maintained within .10 psi. The BRU speed was set by changing the characteristics of the speed controller and was set within 50 rpm of the nominal value.

DISCUSSION

The performance of the BRU 4.25-inch radial compressor is presented in figures 1-9 for the following ranges of test variables:

Rotational speed: 32,400 - 39,600 rpm

Turbine inlet temperature: 1200 - 1600° F

Compressor discharge pressure: 20 - 45 psia

Compressor inlet temperature: 60 - 120° F

The impact of these variables on weight flow and compressor pressure ratio is shown in figures 1-6, and the effects on temperature rise ratio and compressor efficiency are presented in figures 7 and 8 respectively. The equivalent weight flow and compressor speed are presented in figure 9 with compressor efficiency and pressure ratio.

Flow Rate

The effects of compressor discharge pressure on weight flow are shown in figures 1 through 5. The weight flow increases with increasing discharge pressure, (P_{CD}), rotative speed, and with decreasing turbine inlet temperature and compressor inlet temperature. The maximum weight flow of 1.435 lb/sec occurred at a compressor inlet temperature of 60° F, compressor discharge pressure of 45 psia, turbine inlet temperature of 1200° F and 39,600 rpm (fig. 1c).

Compressor Static Pressure Ratio

The compressor static pressures ratios (discharge to inlet, P_{CD}/P_{CI}) obtained are presented in figures 1 through 6. Figures 1 through 5 show the effects of compressor discharge pressure on compressor pressure ratio for constant compressor inlet temperatures whereas figure 6 shows effects of compressor discharge pressure for lines of constant turbine inlet temperature on compressor pressure ratio. The compressor pressure ratio increases with increasing speed and turbine inlet temperature; decreases slightly with increasing discharge pressure and compressor inlet temperature. At a turbine inlet temperature of 1600° F and speed of 36,000 rpm (figure 5b) increasing the compressor inlet temperature from 60° to 120° resulted in a decrease in compressor pressure ratio from approximately 1.96 to approximately 1.82.

Compressor Temperature Rise Ratio

The effects of compressor discharge pressure on compressor temperature rise ratio are presented in figure 7. The temperature rise ratio is

$$\frac{T_{CD} - T_{CI}}{T_{CI}} \quad \text{where}$$

T_{CD} = Compressor discharge temperature

T_{CI} = Compressor inlet temperature

The temperature rise ratio (figure 7) increased with decreasing speed. Compressor discharge pressure and turbine inlet temperature have very little effect on the temperature rise ratio. The increased compressor discharge temperatures due to the BRU insulation resulted in compressor temperature rise ratios which were higher than those calculated during previous tests.

Compressor Efficiency

The effects of compressor discharge pressure on compressor efficiency, η_c , are presented in figure 8. The efficiency is defined as:

$$\eta_c = \frac{T_{CI} \left[\left(\frac{P_{CD}}{P_{CI}} \right)^{0.4} - 1 \right]}{T_{CD} - T_{CI}}$$

where

T_{CI} = Compressor inlet temperature, °R

P_{CD} = Compressor discharge pressure, psia

P_{CI} = Compressor inlet pressure, psia

T_{CD} = Compressor discharge temperature, °R

The compressor efficiency (figure 8) increased slightly with increasing discharge pressure and turbine inlet temperature. The efficiency decreased with increasing compressor inlet temperature and with speed (figure 8). The indicated efficiency varied from approximately 69 to 75 percent during the test. The efficiencies observed during the test were lower than those calculated during previous tests. As mentioned in the apparatus section, the BRU was insulated. This reduced the heat loss and increased the compressor discharge temperature, resulting in lower calculated efficiencies.

Standardized Compressor Data

The data shown in figure 9 are presented in the conventional method used in compressor studies. The effects of equivalent weight flow $\frac{W}{\sqrt{A}}$ on compressor efficiency, pressure ratio, and equivalent speed are shown. The data are plotted for constant ratios of constant turbine inlet temperature to compressor inlet temperature for the range of turbine inlet temperature from 1200 to 1600° F. As the equivalent weight flow is increased, the compressor equivalent speed and pressure ratio increase. The compressor efficiency shows only a slight variation over the entire range.

CONCLUDING REMARKS

The performance characteristics of a 4.5-inch radial compressor, as part of the BRU, using He-Xe gas were obtained during operation of a Brayton cycle power system. The test parameters included a range of compressor inlet temperatures, turbine inlet temperatures, compressor discharge pressures and rotative speeds. These test parameters were independently varied to obtain pressure ratio, weight flow, temperature rise ratio and efficiency characteristics of the compressor.

The preliminary results of the experimentation showed:

1. Compressor static pressure ratio increased with increasing rotational speed and turbine inlet temperature but decreased with increasing compressor inlet temperature. Compressor pressure ratio was not significantly affected by compressor discharge pressure.
2. Compressor weight flow changes linearly with compressor discharge pressure over the experimental range. Small increases in weight flow were observed with decreasing compressor inlet temperature, with increasing rotational speed and turbine inlet temperature.
3. Decreasing the compressor inlet temperature and/or increasing the rotational speed produced an increase in the temperature rise ratio. Compressor discharge pressure and turbine inlet temperature had virtually no effect on the compressor temperature rise ratio.
4. Compressor efficiency was slightly affected by rotational speed; large increases in compressor efficiency resulted by decreasing compressor inlet temperature. Turbine inlet temperature effect on efficiency was insignificant.

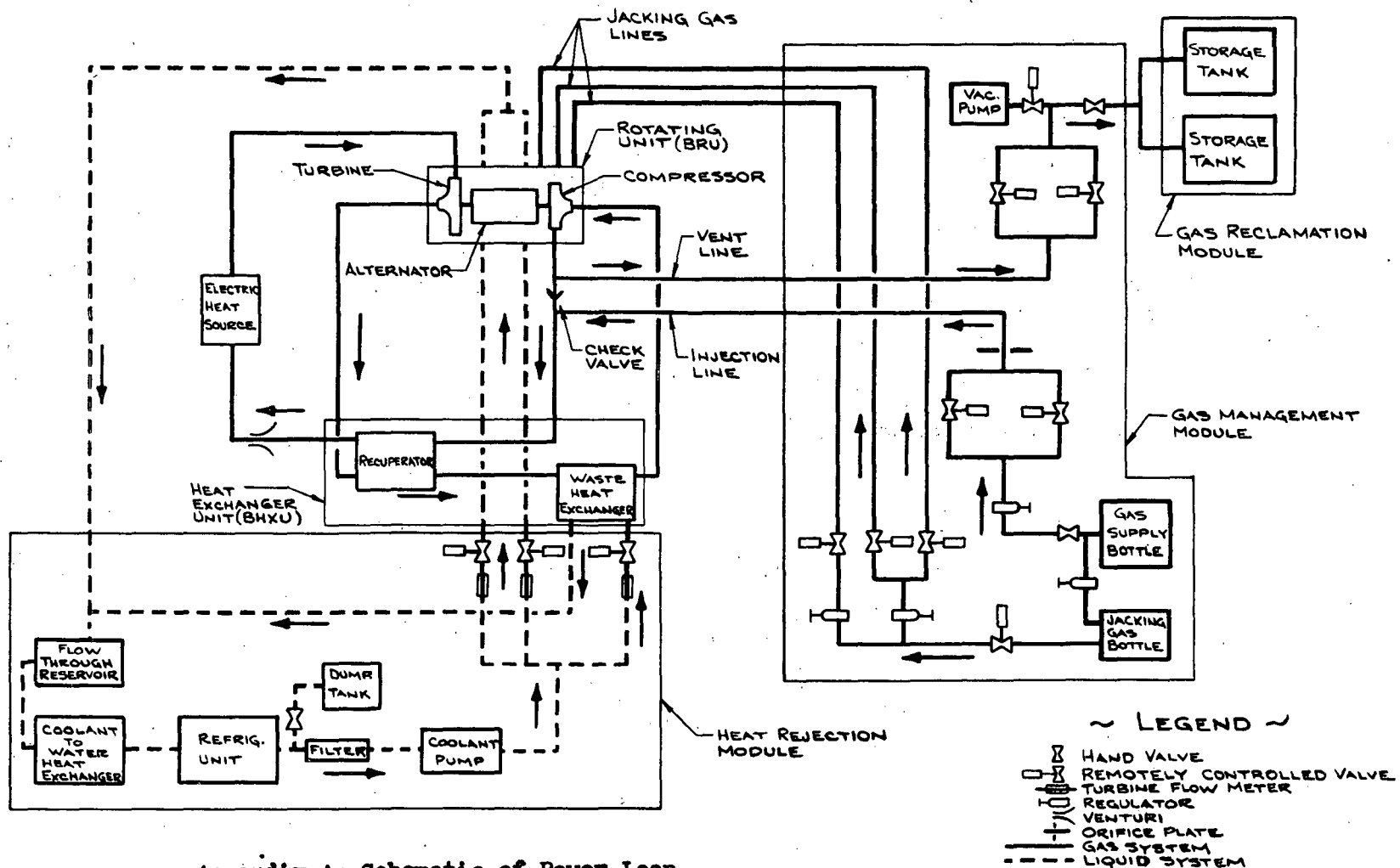
Lewis Research Center,
National Aeronautics and Space Administration,
Cleveland, Ohio, December 14, 1971.

REFERENCES

1. Klann, John L.; Wintucky, William T.: Status of the 2-to-15 kWe Brayton Power System and Potential Gains from Component Improvements. NASA TM X-67835, 1971.
2. Wong, Robert Y.; Klassen, Hugh A.; Evans, Robert C.; and Winzig, Charles H.: Preliminary Investigation of a Single-Shaft Brayton Rotating Unit Designed for a 2-to-10 Kilowatt Space Power Generation System. NASA TM X-1869, 1969.
3. Valerino, Alfred S.; Macosko, Robert P.; Asadourian, Armen S.; Hecker, Thomas P.; and Kruchowy, Roman: Preliminary Performance of a Brayton-Cycle-Power-System Gas Loop Operating with Krypton Over a Turbine Inlet Temperature Range of 1200^oF to 1600^oF. NASA TM X-52769, 1970.
4. Vernon, Richard W.; and Miller, Thomas J.: Experimental Performance of a 2-15 Kilowatt Brayton Power System Using a Mixture of Helium and Xenon. NASA TM X-52936, 1970.
5. Valerino, Alfred S.; and Ream, Lloyd W.: Performance of a Brayton-Cycle Power Conversion System Using a Helium-Xenon Gas Mixture. NASA TM X-67846, 1971.
6. Weigel, Carl, Jr.; Tysl, Edward R.; and Ball, Calvin L.: Overall Performance in Argon of 4.25 Inch Sweptback-Bladed Centrifugal Compressor. NASA TM X-2129, 1970.
7. Anon: Design and Fabrication of the Brayton Cycle High Performance Compressor Research Package. Final Report, NASA CR-72533, 1967.

TABLE I. - COMPRESSOR DESIGN PARAMETERS

| | |
|---|--------|
| Working fluid, HeXe mixture with molecular weight of nominal 83.8 | |
| Inlet total pressure, P_1 , psia; | 13.5 |
| Inlet total temperature, T_1 , °R | 540 |
| Weight flow rate, W , lb/sec | 0.756 |
| Compressor total-pressure ratio, P_6/P_1 | 1.9 |
| Compressor total-temperature ratio, T_6/T_1 | 1.37 |
| Compressor efficiency, 1-6 | 0.80 |
| Impeller total-pressure ratio, P_3/P_1 | 2.03 |
| Impeller efficiency, 1-3 | 0.895 |
| Rotative speed, RPM | 36 000 |
| Impeller tip speed, U_{t3} , ft/sec | 667 |
| Specific speed, N_s | 0.11 |



Appendix A: Schematic of Power Loop

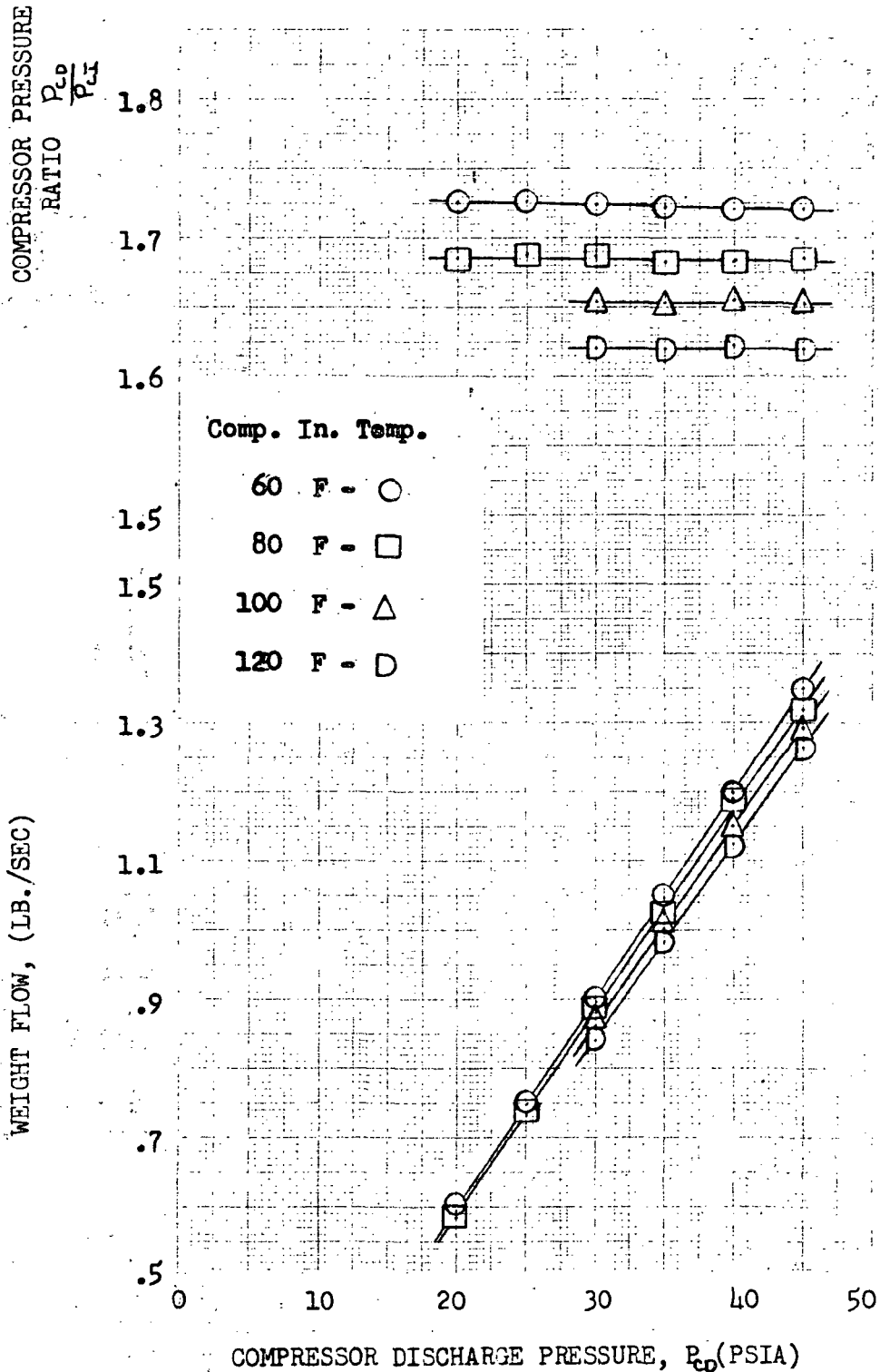


Figure 1: Effect of Compressor Discharge Pressure on Compressor Pressure Ratio, and Weight Flow using Helium-Xenon Gas at a Turbine Inlet Temperature of 1200 F.
 (a) Rotational Speed 32,400 RPM.

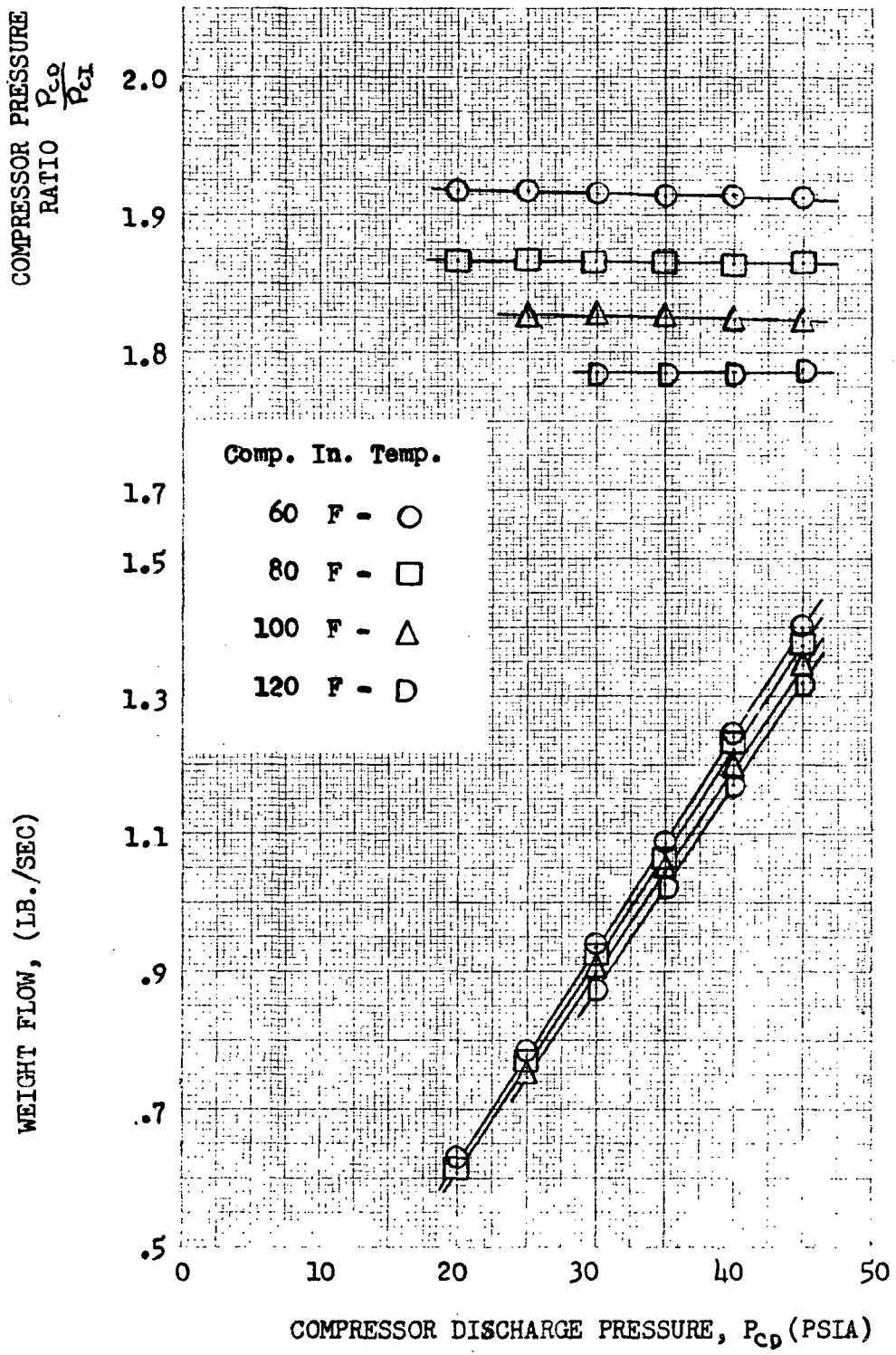


Figure 1: Effect of Compressor Discharge Pressure on Compressor Pressure Ratio, and Weight Flow Using Helium-Xenon Gas at a Turbine Inlet Temperature of 1200 F
 (b) Rotational Speed 36,000 RPM.

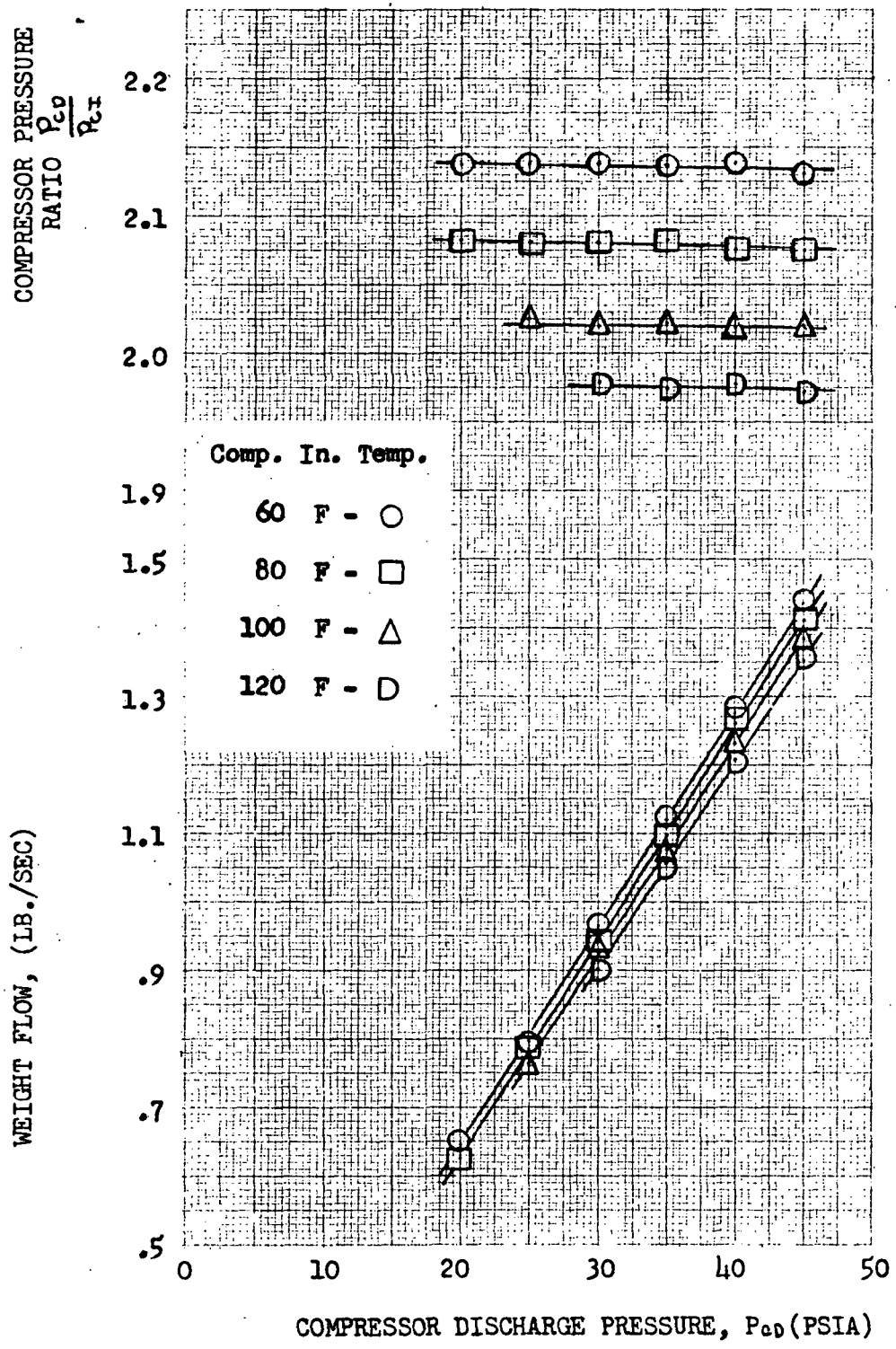


Figure 1. Effect of Compressor Discharge Pressure on Compressor Pressure Ratio, and Weight Flow Using Helium-Xenon Gas at a Turbine Inlet Temperature of 1200 F (c) Rotational Speed 39,600 RPM.

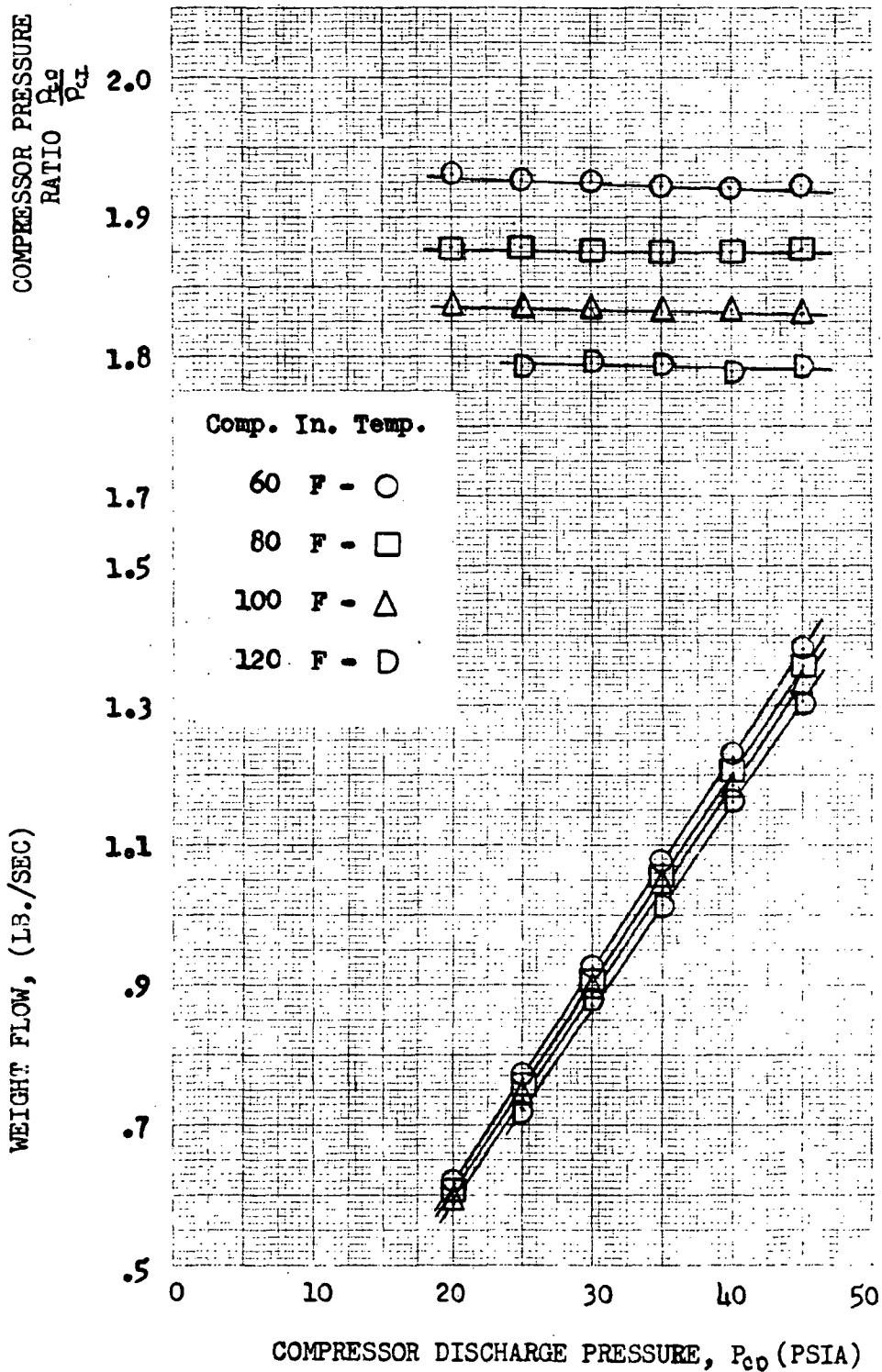


Figure 2: Effect of Compressor Discharge Pressure on Compressor Pressure Ratio, and Weight Flow using Helium-Xenon Gas at a Turbine Inlet Temperature of 1300 F and Rotational Speed of 36,000 RPM.

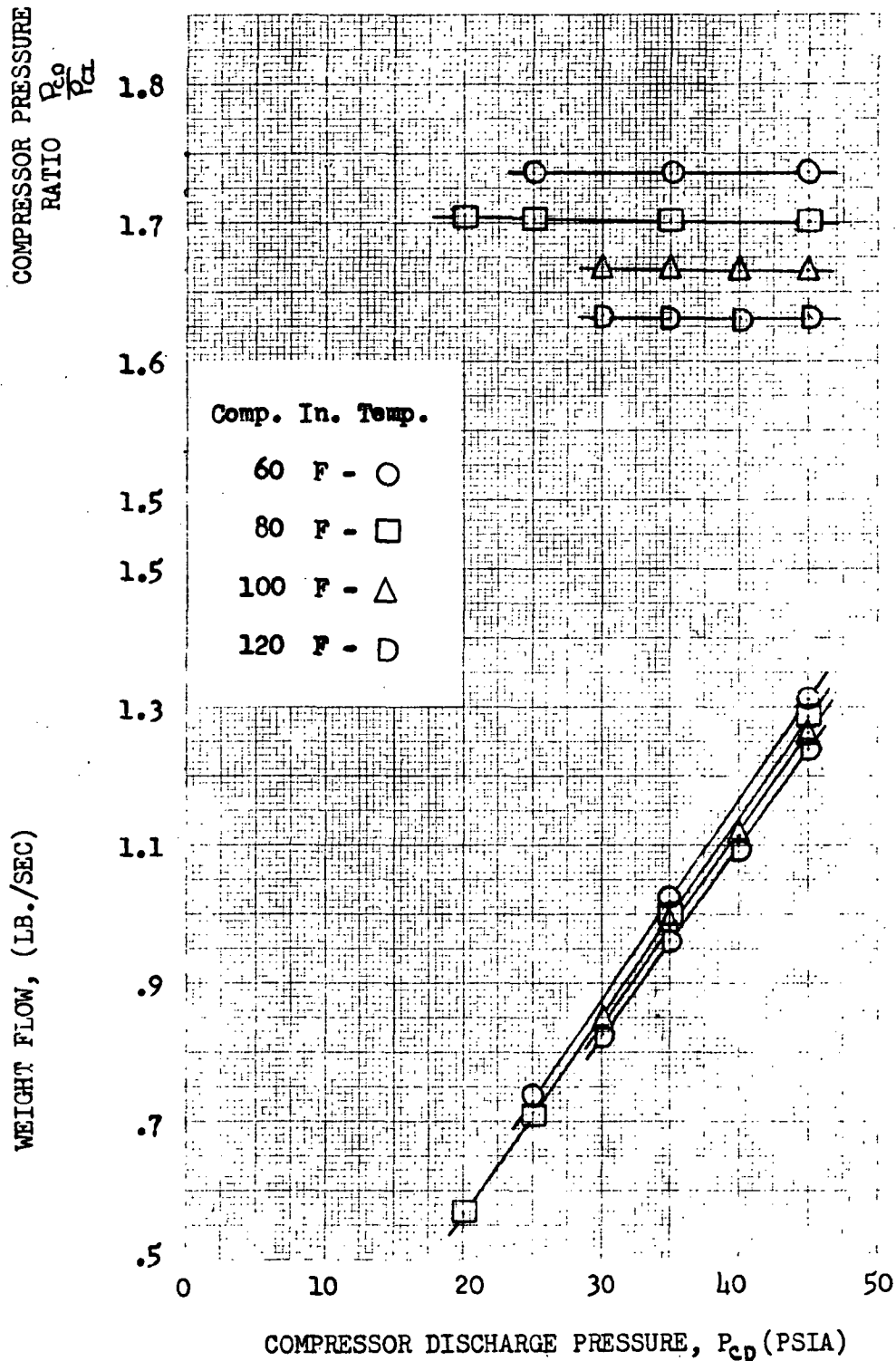


Figure 3: Effect of Compressor Discharge Pressure on Compressor Pressure Ratio, and Weight Flow using Helium-Xenon Gas at a Turbine Inlet Temperature of 1400 F.
 (a) Rotational Speed 32,400 RPM.

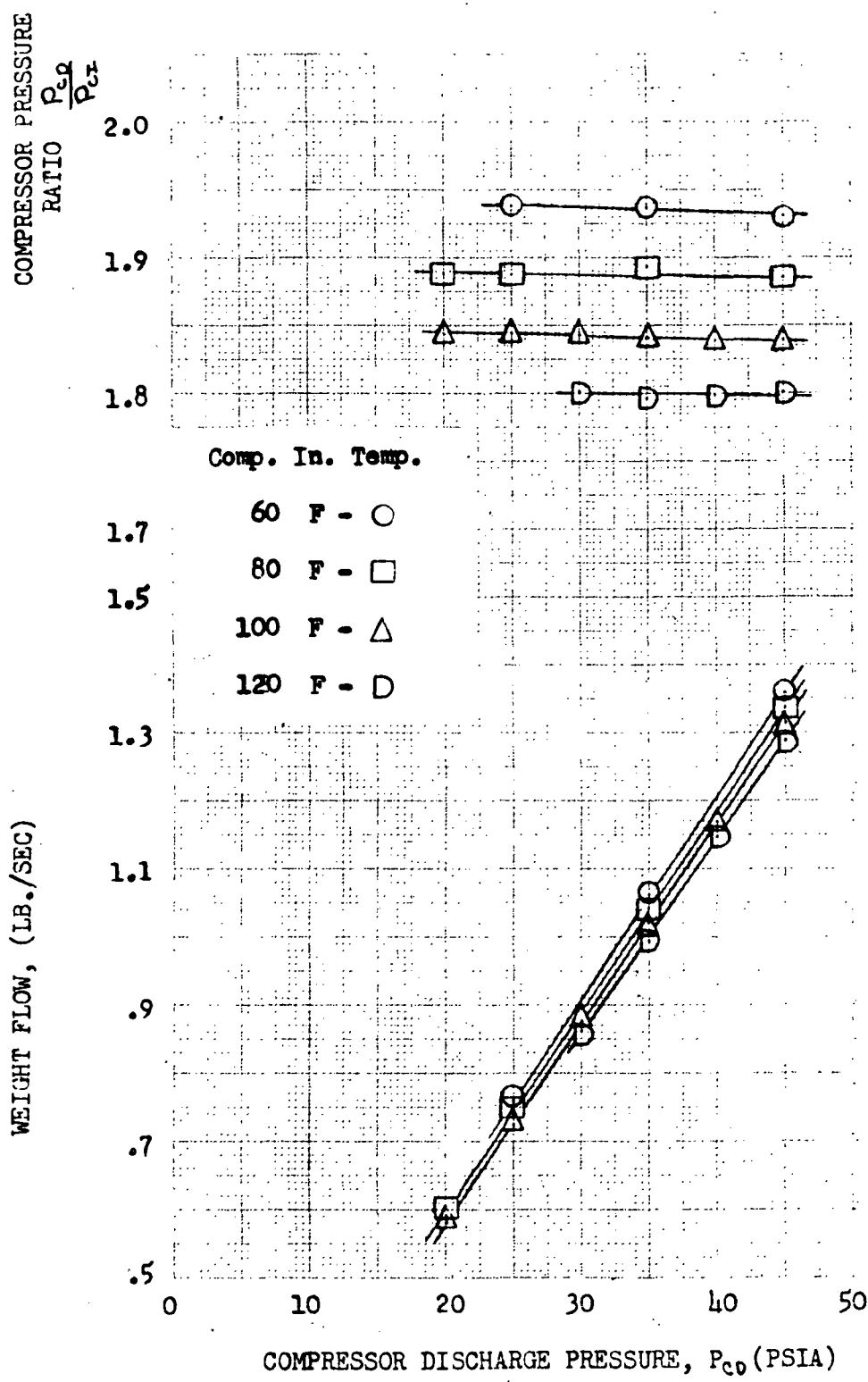


Figure 3: Effect of Compressor Discharge Pressure on Compressor Pressure Ratio, and Weight Flow using Helium-Xenon Gas at a Turbine Inlet Temperature of 1400 F.
 (b) Rotational Speed 36,000 RPM.

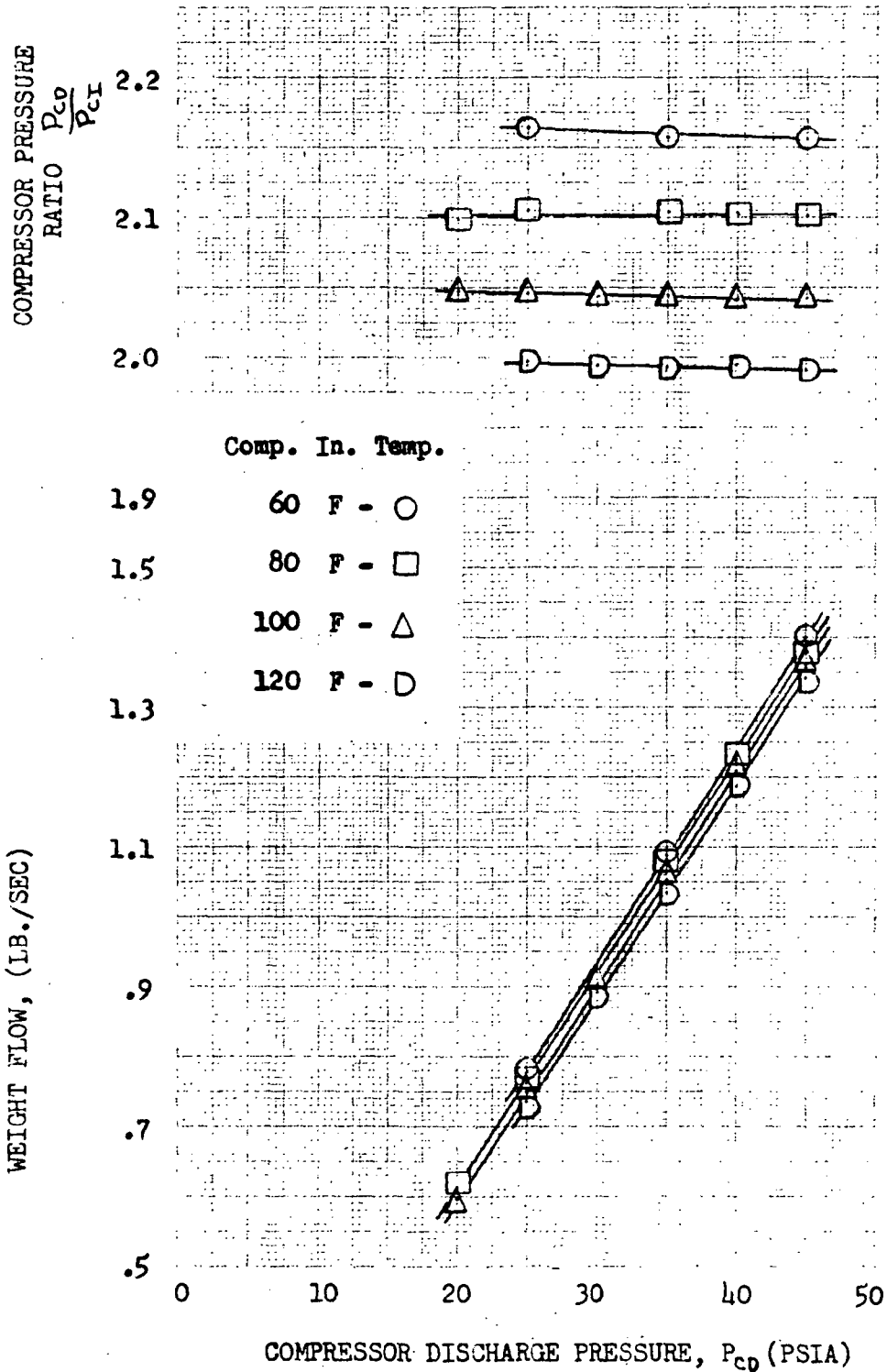


Figure 3: Effect of Compressor Discharge Pressure on Compressor Pressure Ratio, and Weight Flow using Helium-Xenon Gas at a Turbine Inlet Temperature of 1400 F.
 (c) Rotational Speed 39,600 RPM.

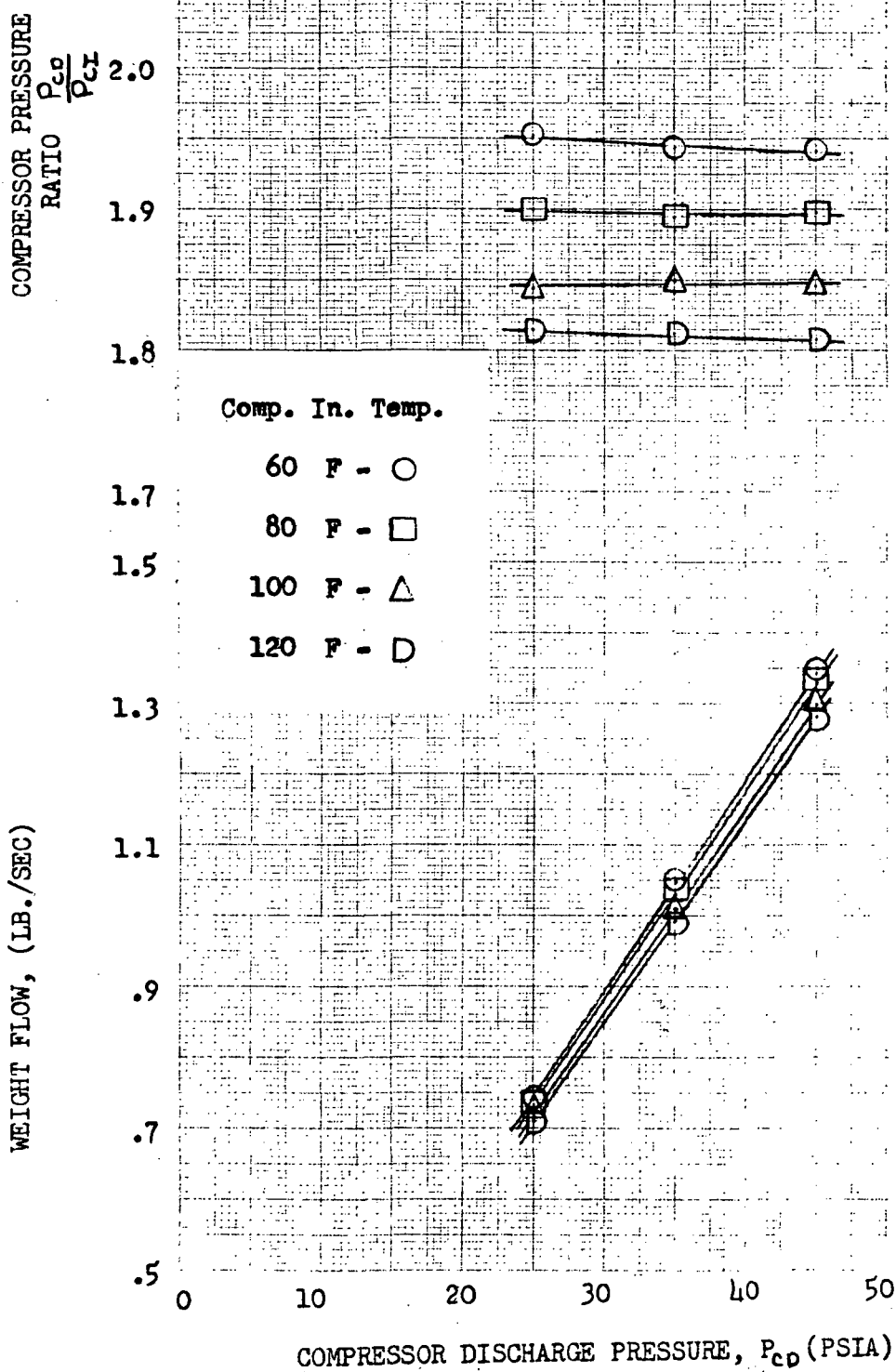


Figure 4: Effect of Compressor Discharge Pressure on Compressor Pressure Ratio, and Weight Flow using Helium-Xenon Gas at a Turbine Inlet Temperature of 1500 F and Rotational Speed of 36,000 RPM.

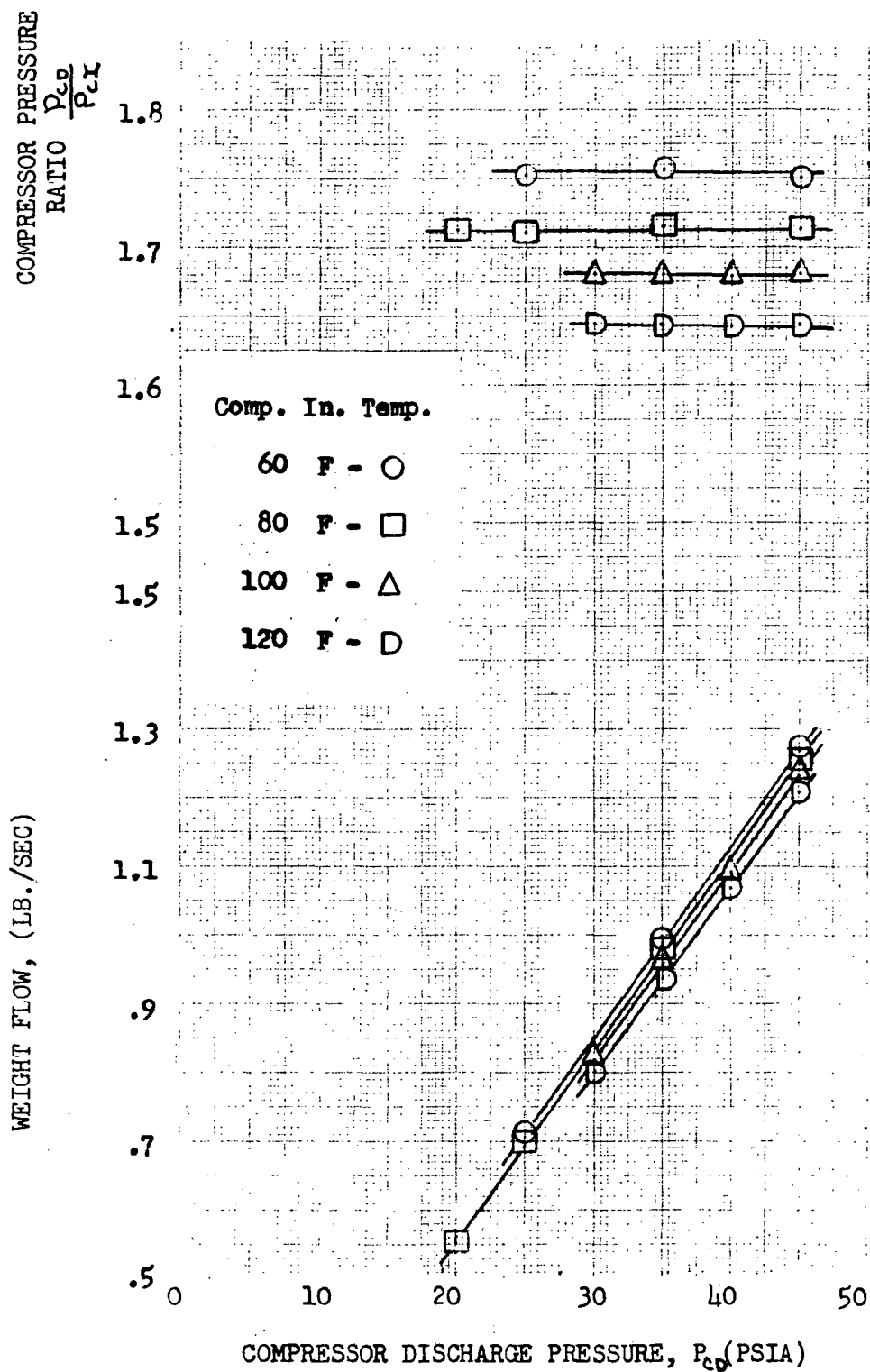


Figure 5: Effect of Compressor Discharge Pressure on Compressor Pressure Ratio, and Weight Flow using Helium-Xenon Gas at a Turbine Inlet Temperature of 1600 F.
 (a) Rotational Speed 32,400 RPM.

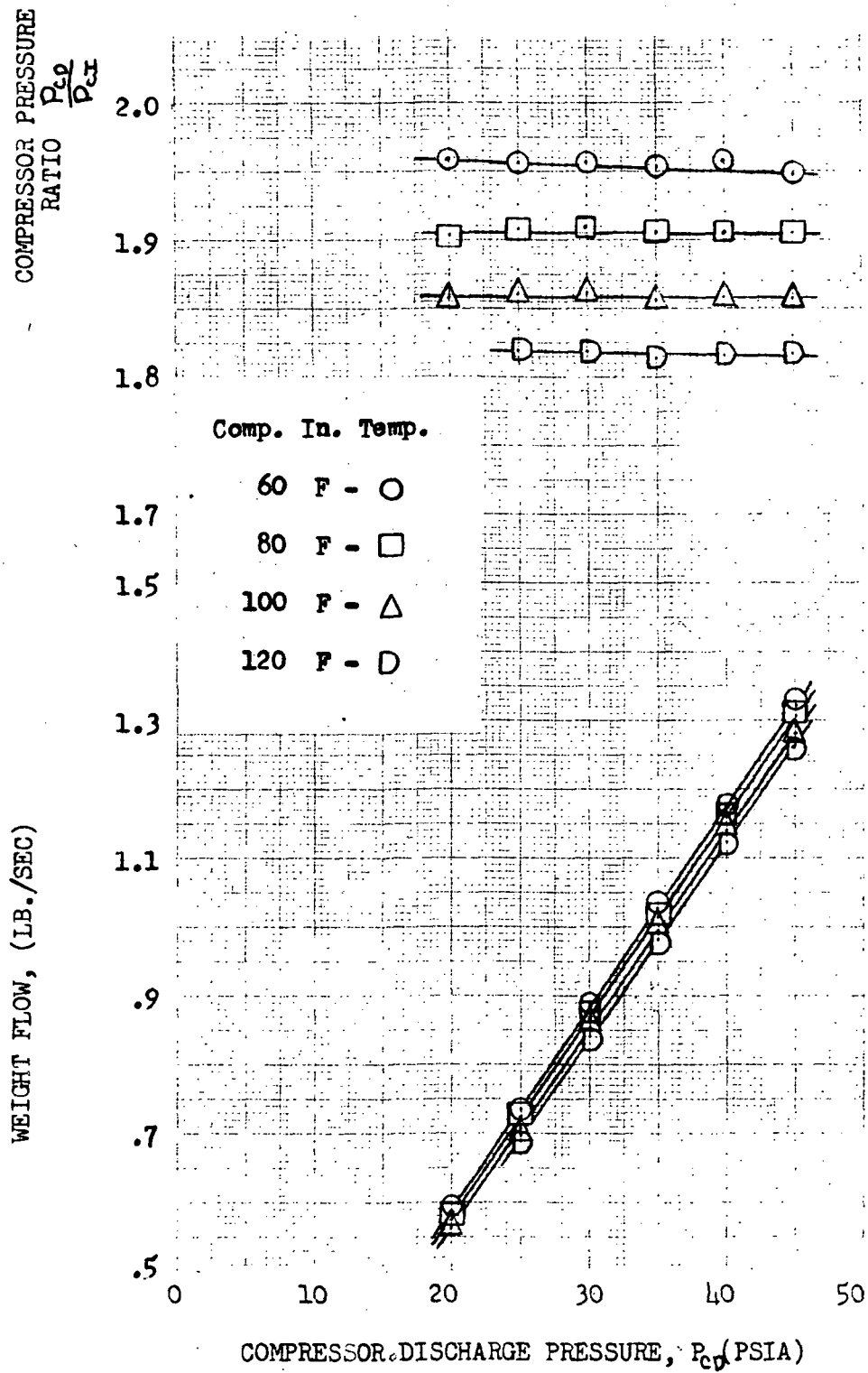


Figure 5: Effect of Compressor Discharge Pressure on Compressor Pressure Ratio, and Weight Flow using Helium-Xenon Gas at a Turbine Inlet Temperature of 1600 F.
 (b) Rotational Speed 36,000 RPM.

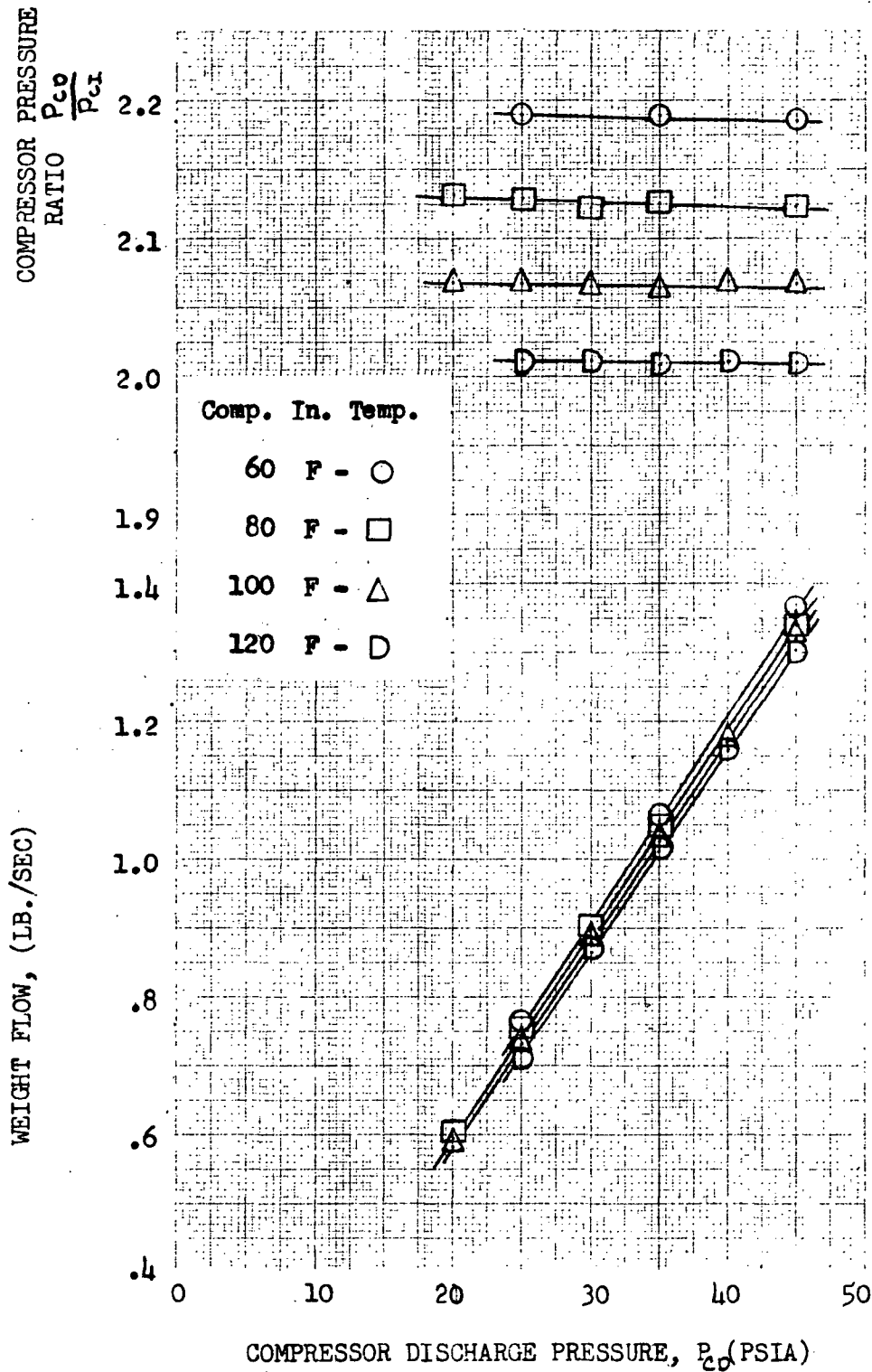


Figure 5: Effect of Compressor Discharge Pressure on Compressor Pressure Ratio, and Weight Flow using Helium-Xenon Gas at a Turbine Inlet Temperature of 1600 F.
 (c) Rotational Speed 39,600 RPM.

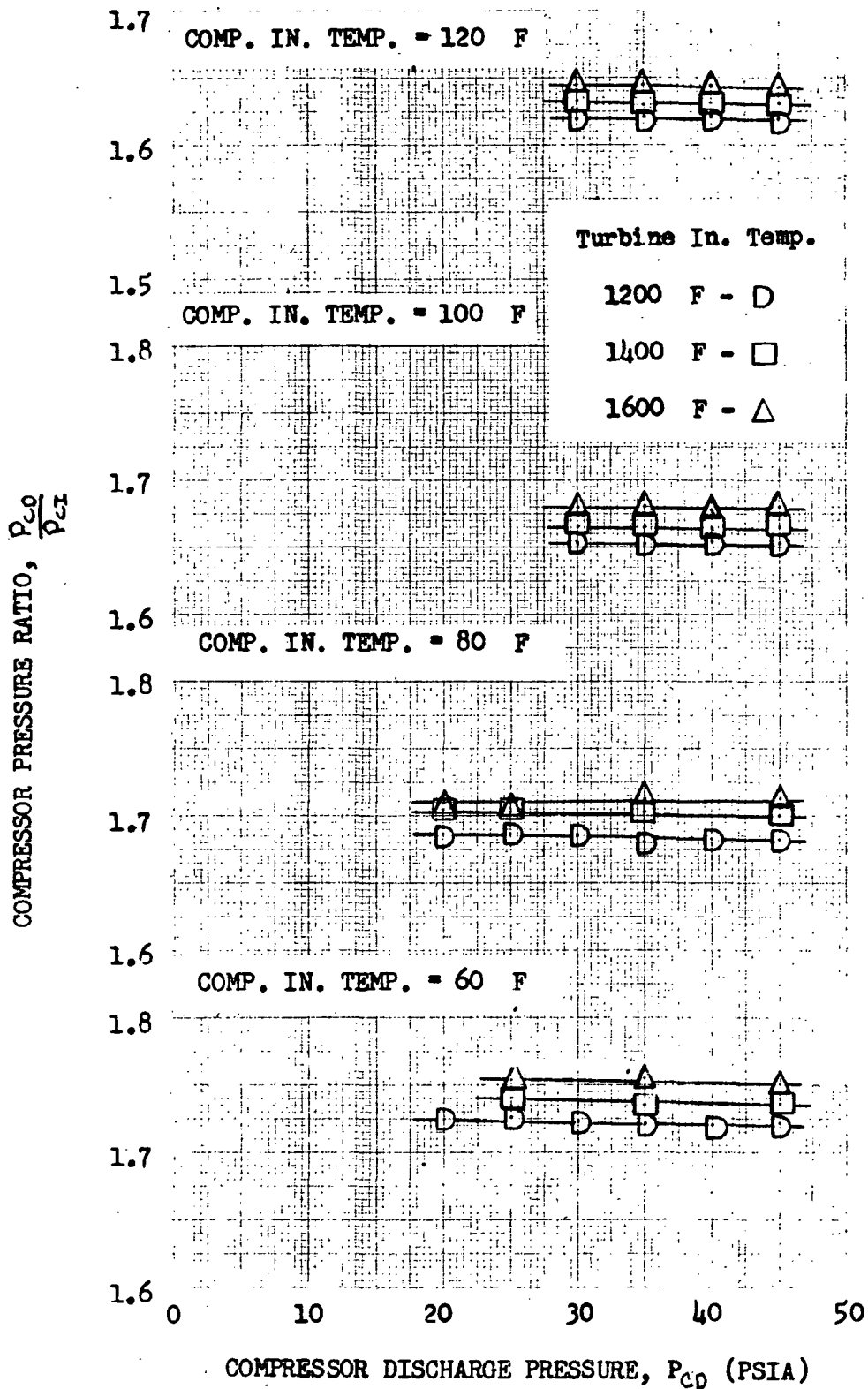


Figure 6: Effect of Compressor Discharge Pressure on Compressor Pressure Ratio For Compressor Inlet Temperatures of 60 F, 80 F, 100 F, and 120 F using Helium-Xenon Gas.
 (a) Rotational Speed 32,400

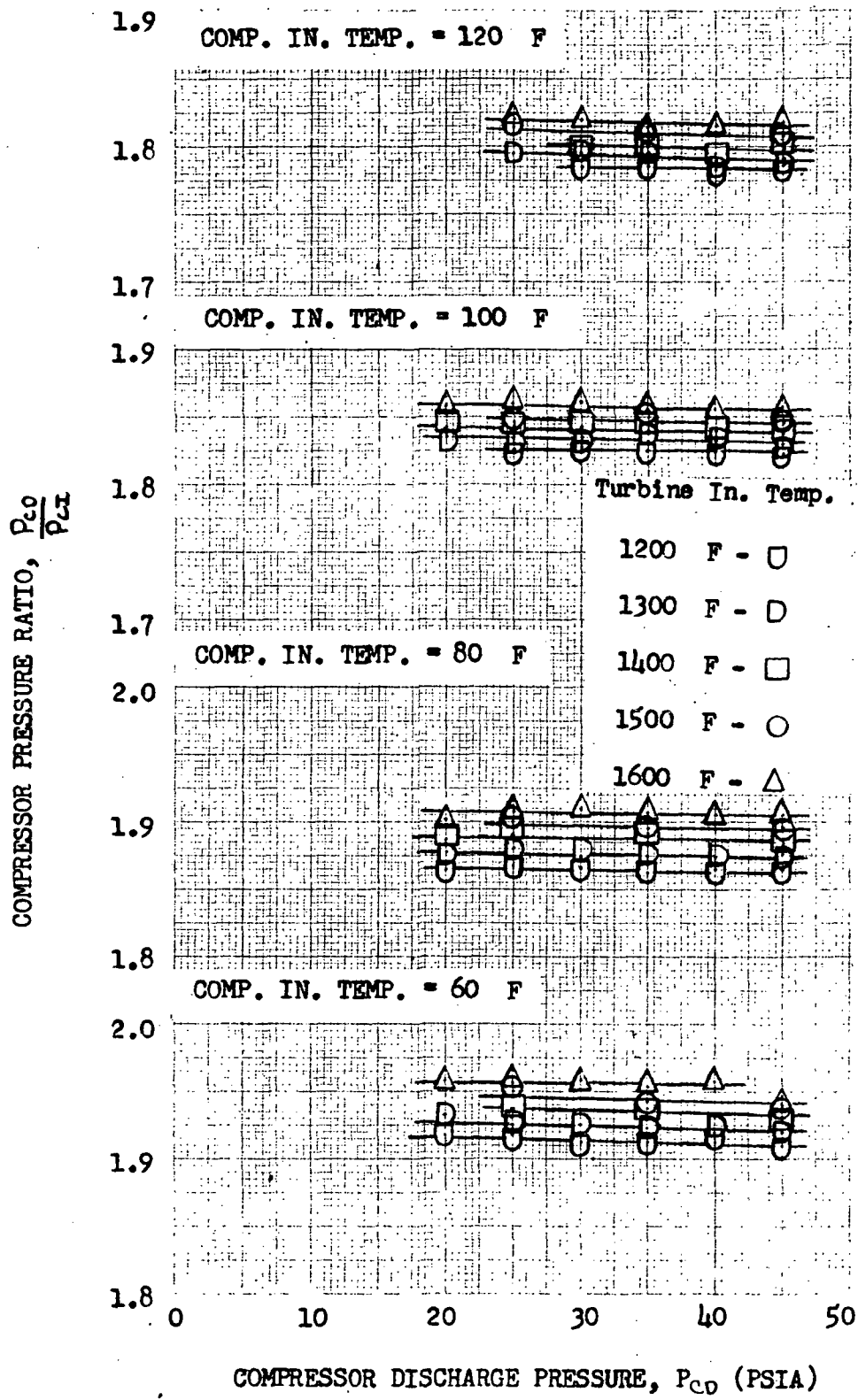


Figure 6: Effect of Compressor Discharge Pressure on Compressor Pressure Ratio for Compressor Inlet Temperatures of 60 F, 80 F, 100 F, and 120 F using Helium-Xenon Gas. (b) Rotational Speed 36,000

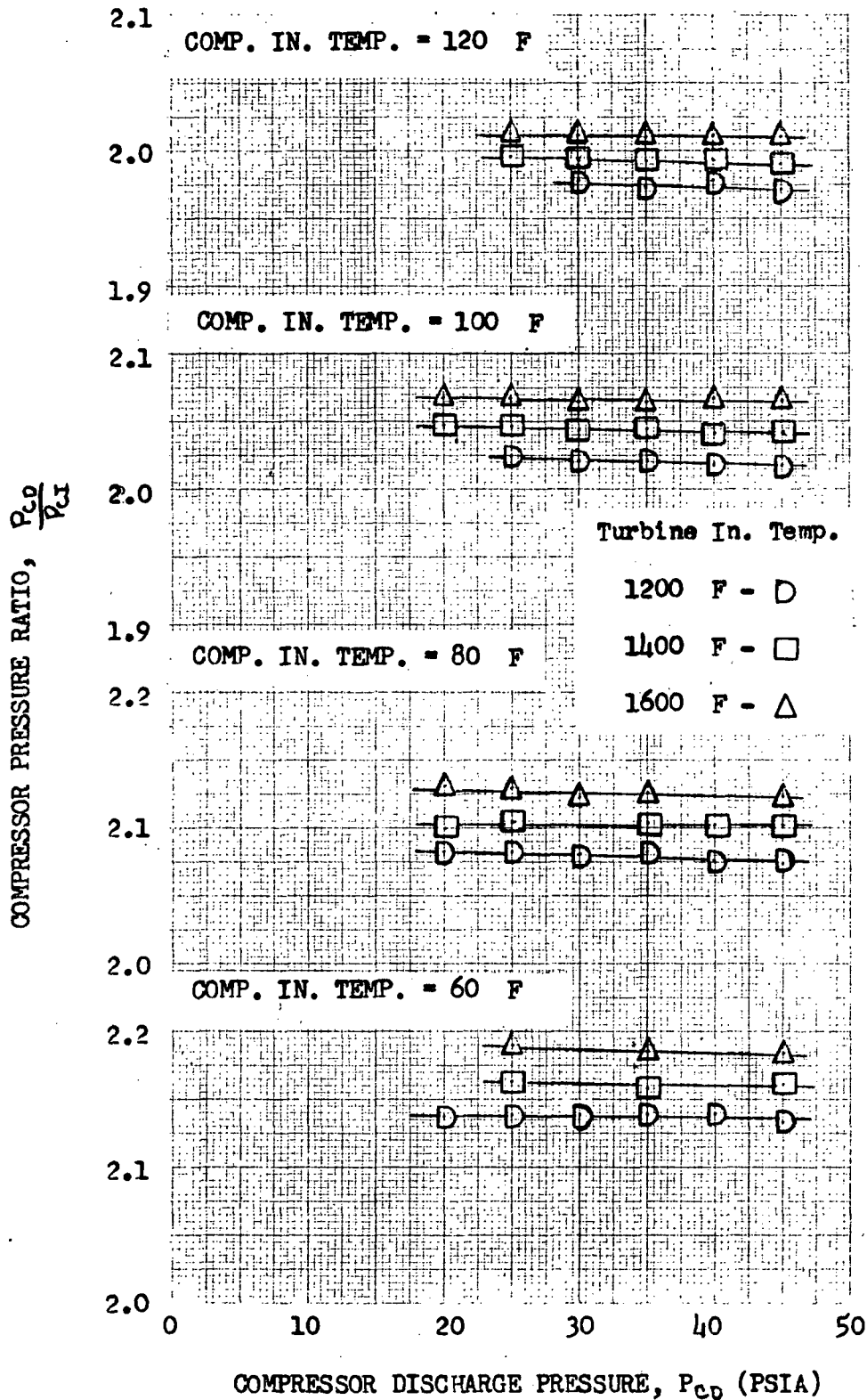


Figure 6: Effect of Compressor Discharge Pressure on Compressor Pressure Ratio For Compressor Inlet Temperatures of 60 F, 80 F, 100 F, and 120 F using Helium-Xenon Gas. (e) Rotational Speed 39,600

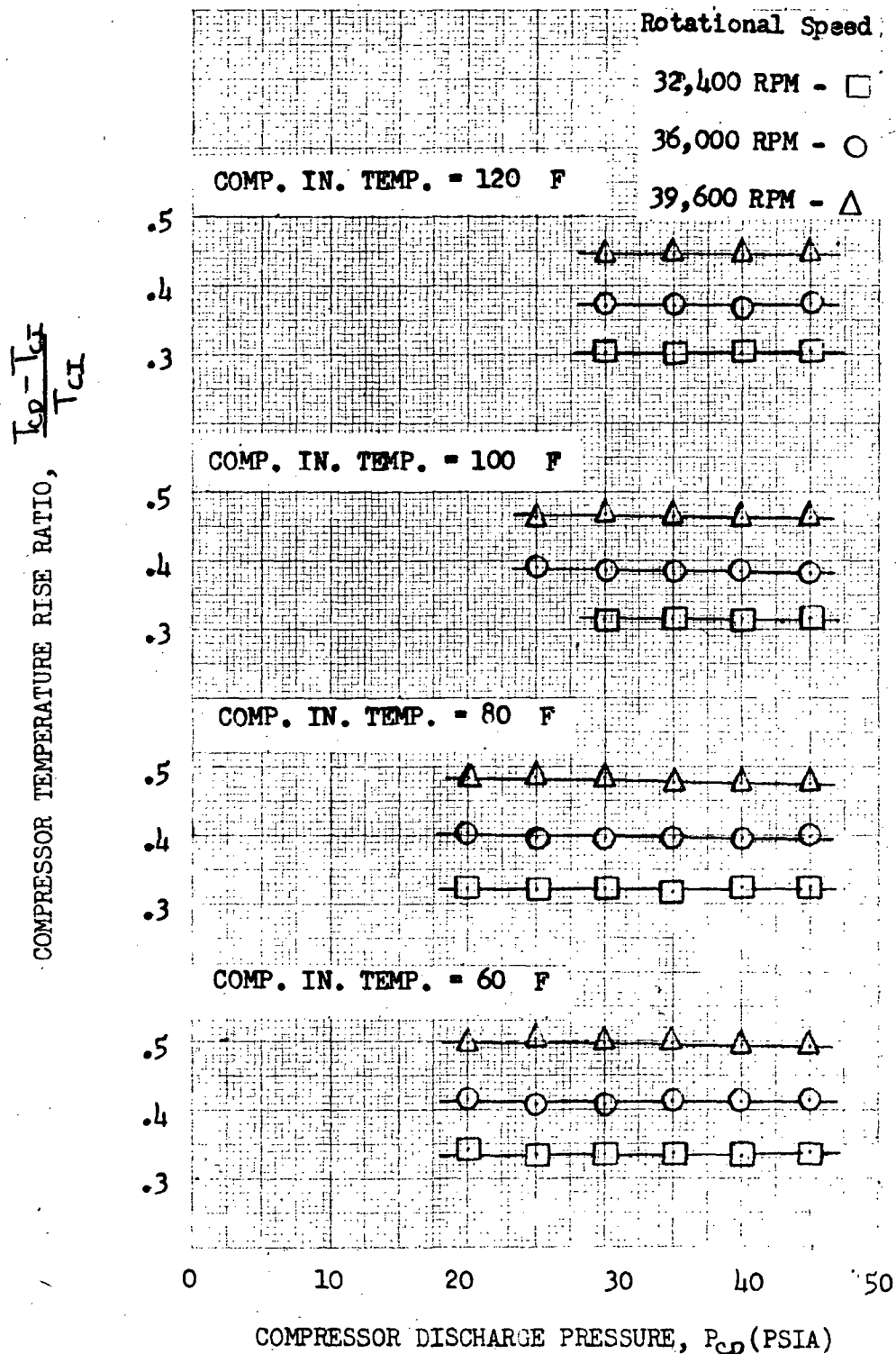


Figure 7: Effect of Compressor Discharge Pressure on the Compressor Temperature Rise Ratio at Compressor Inlet Temperatures of 60 F, 80 F, 100 F, and 120 F using Helium-Xenon Gas.
 (a) Turbine Inlet Temperature 1200 F

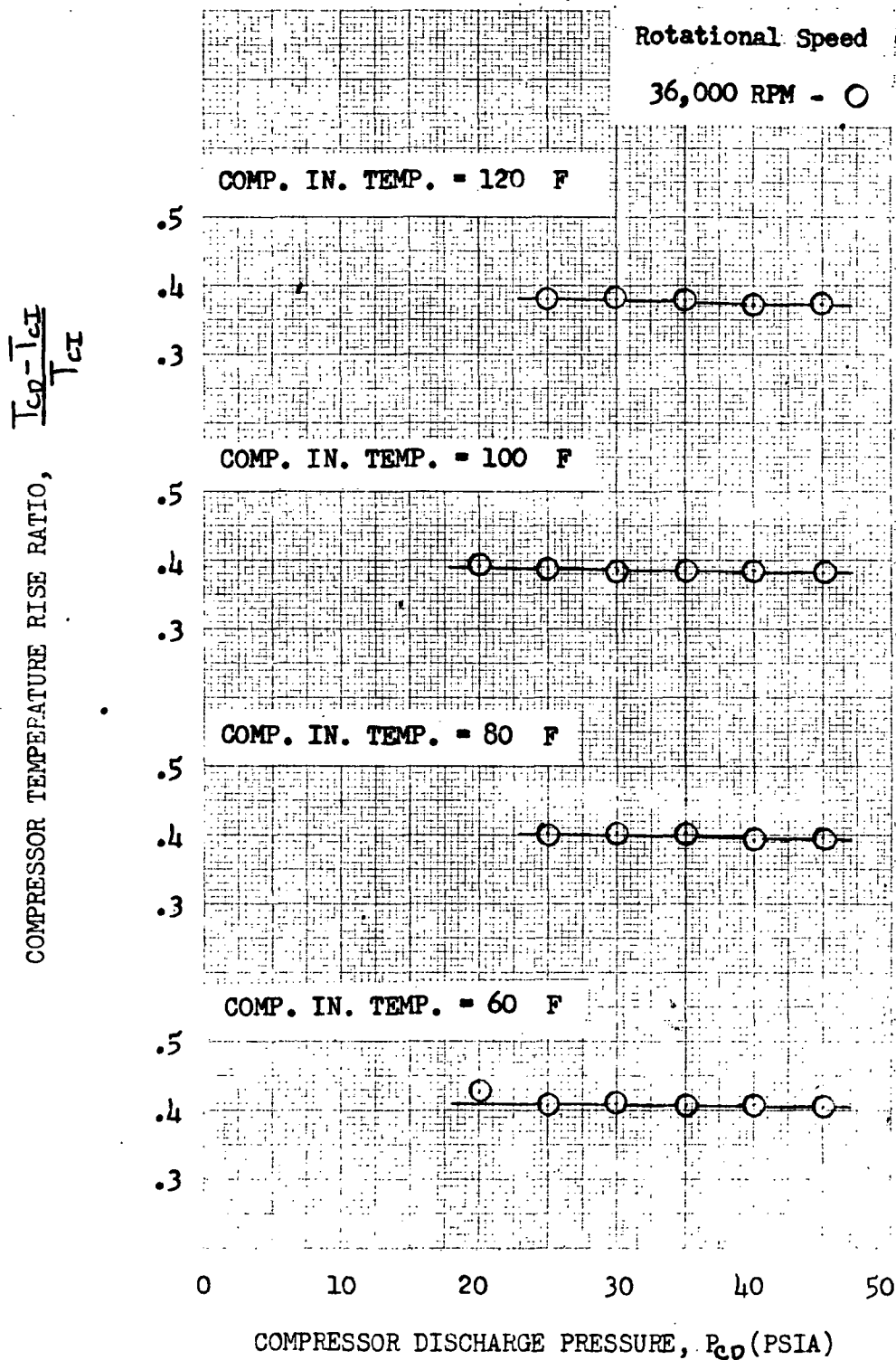


Figure 7: Effect of Compressor Discharge Pressure on the Compressor Temperature Rise Ratio at Compressor Inlet Temperatures of 60 F, 80 F, 100 F, and 120 F using Helium-Xenon Gas.
(b) Turbine Inlet Temperature 1300 F

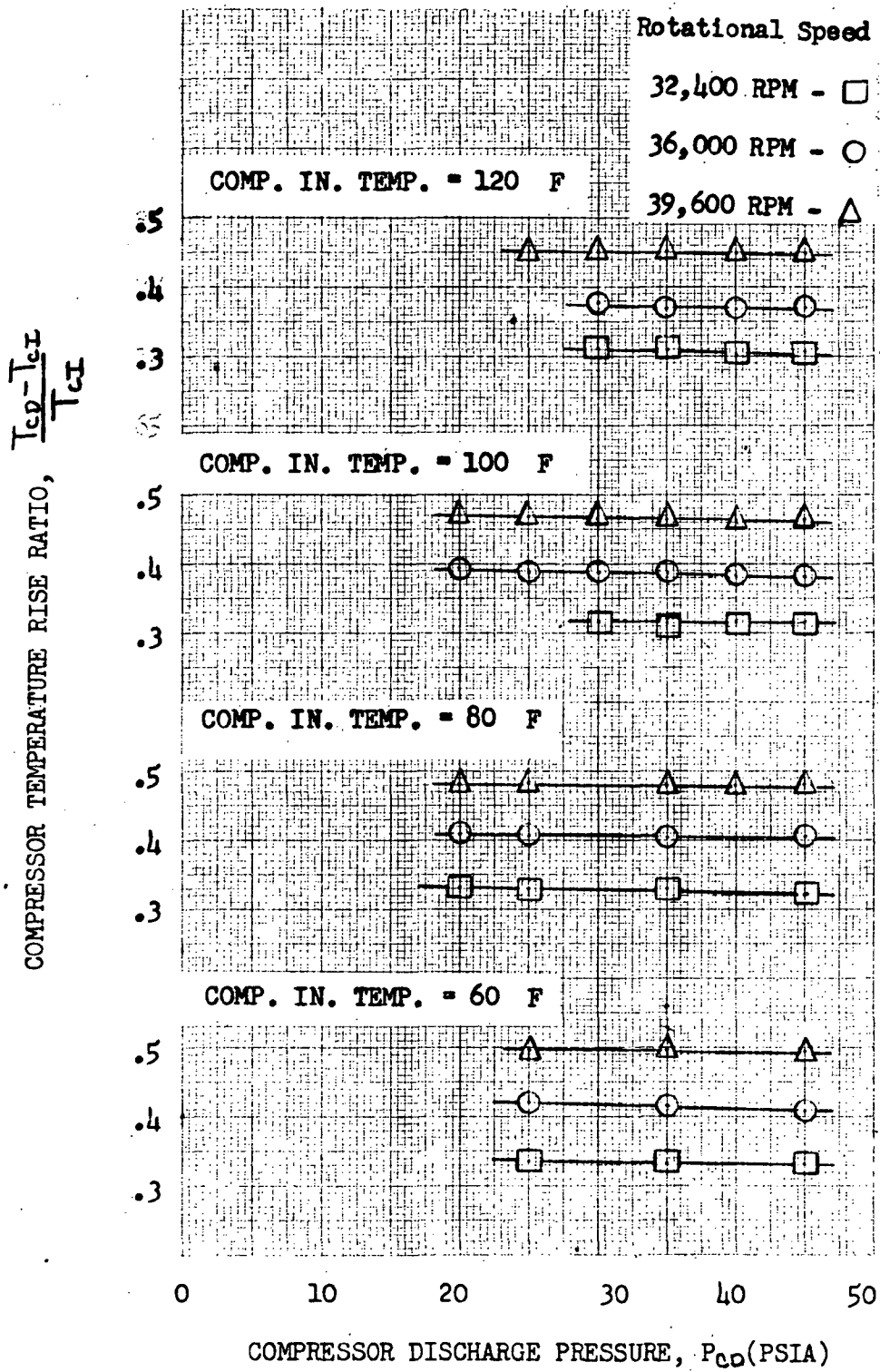


Figure 7: Effect of Compressor Discharge Pressure on the Compressor Temperature Rise Ratio at Compressor Inlet Temperatures of 60 F, 80 F, 100 F, and 120 F using Helium-Xenon Gas. (c) Turbine Inlet Temperature 1400 F

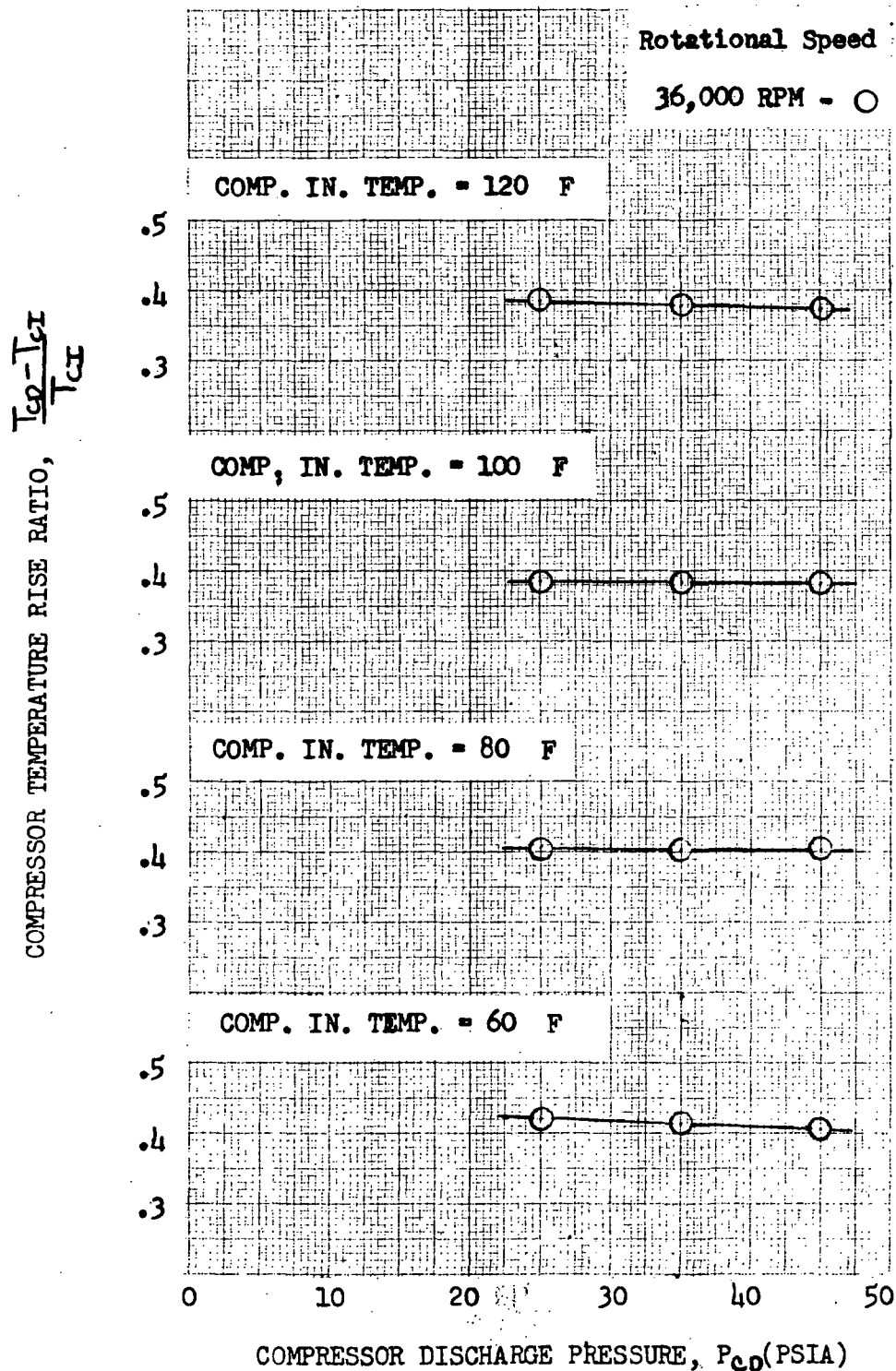


Figure 7: Effect of Compressor Discharge Pressure on the Compressor Temperature Rise Ratio at Compressor Inlet Temperatures of 60 F, 80 F, 100 F, and 120 F using Helium-Xenon Gas.
(d) Turbine Inlet Temperature 1500 F

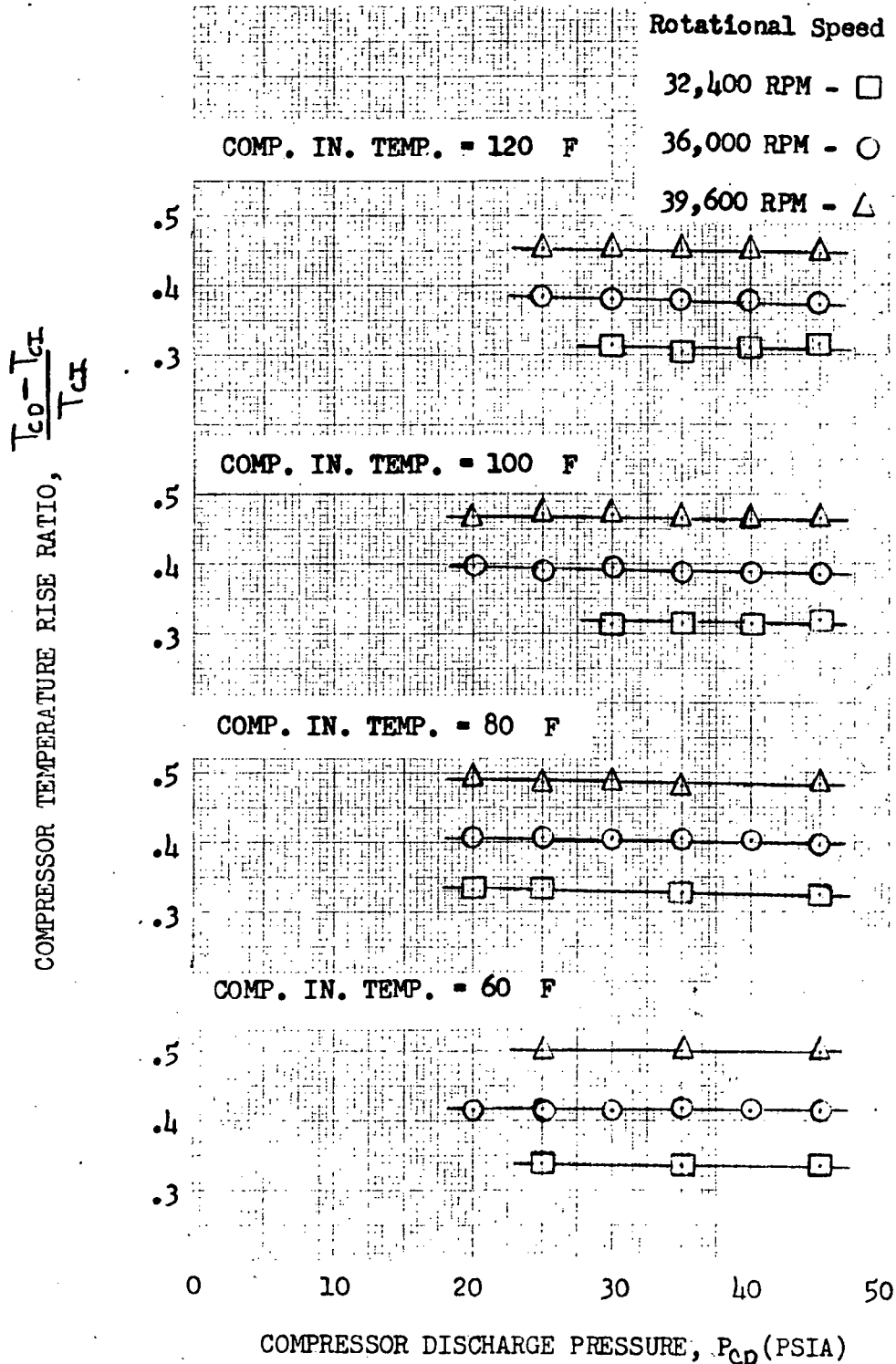


Figure 7: Effect of Compressor Discharge Pressure on the Compressor Temperature Rise Ratio at Compressor Inlet Temperatures of 60 F, 80 F, 100 F, and 120 F using Helium-Xenon Gas. (e) Turbine Inlet Temperature 1600 F

COMPRESSOR EFFICIENCY, γ_c (%)

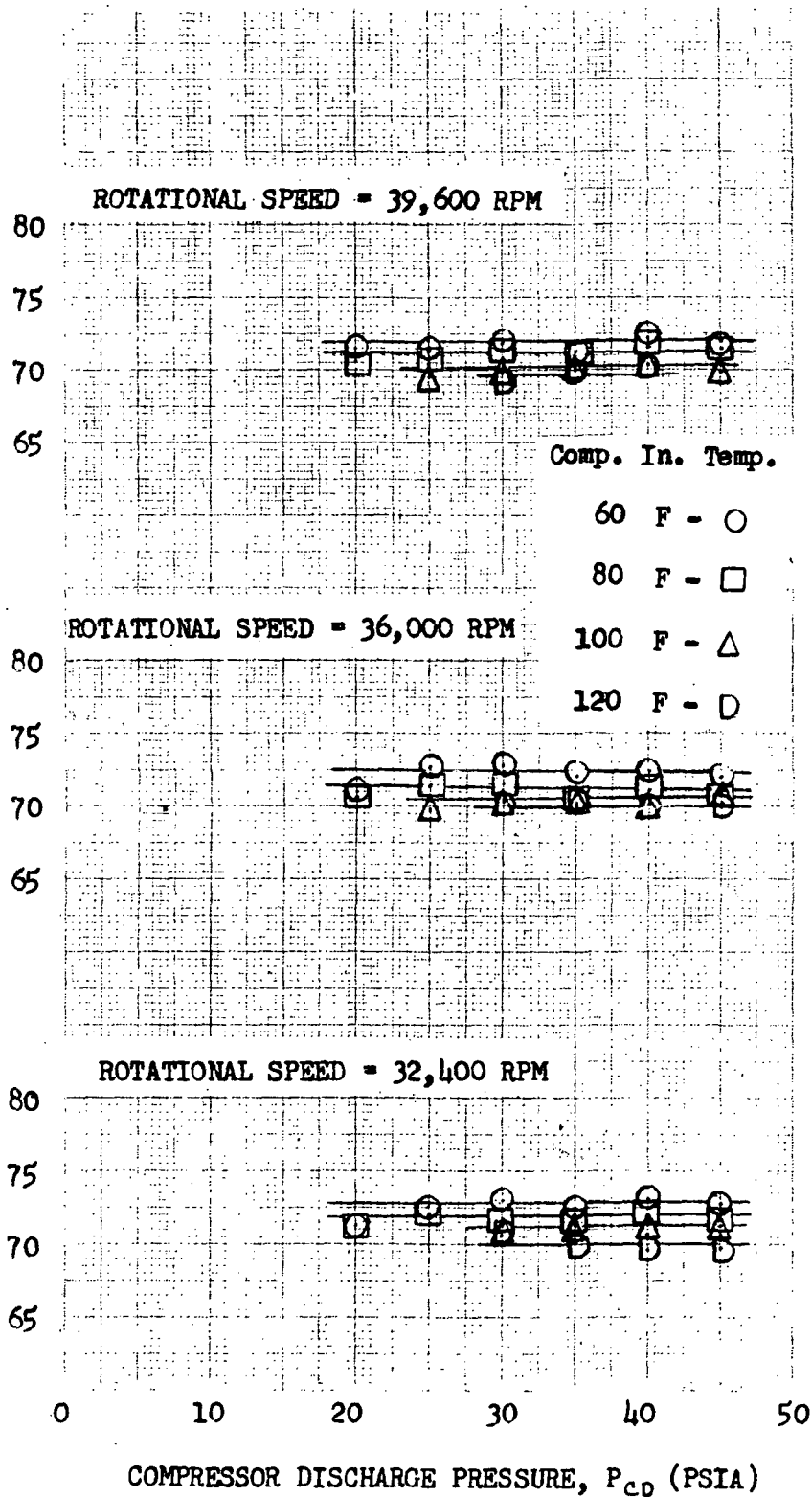


Figure 8: Effect of Compressor Discharge Pressure on Compressor Efficiency at Rotational Speeds of 32,400, 36,000, and 39,600 RPM Using Helium-Xenon Gas.
 (a) Turbine Inlet Temperature 1200 F

COMPRESSOR EFFICIENCY, η_c (%)

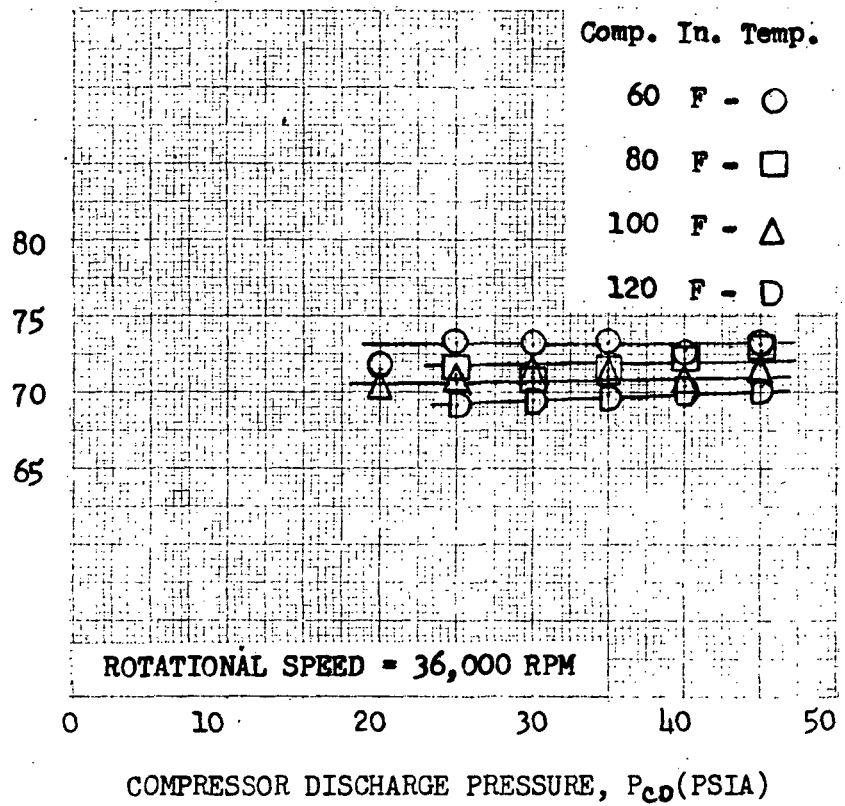


Figure 8: Effect of Compressor Discharge Pressure on Compressor Efficiency at a Rotational Speed of 36,000 RPM using Helium-Xenon Gas.
(b) Turbine Inlet Temperature 1300 F

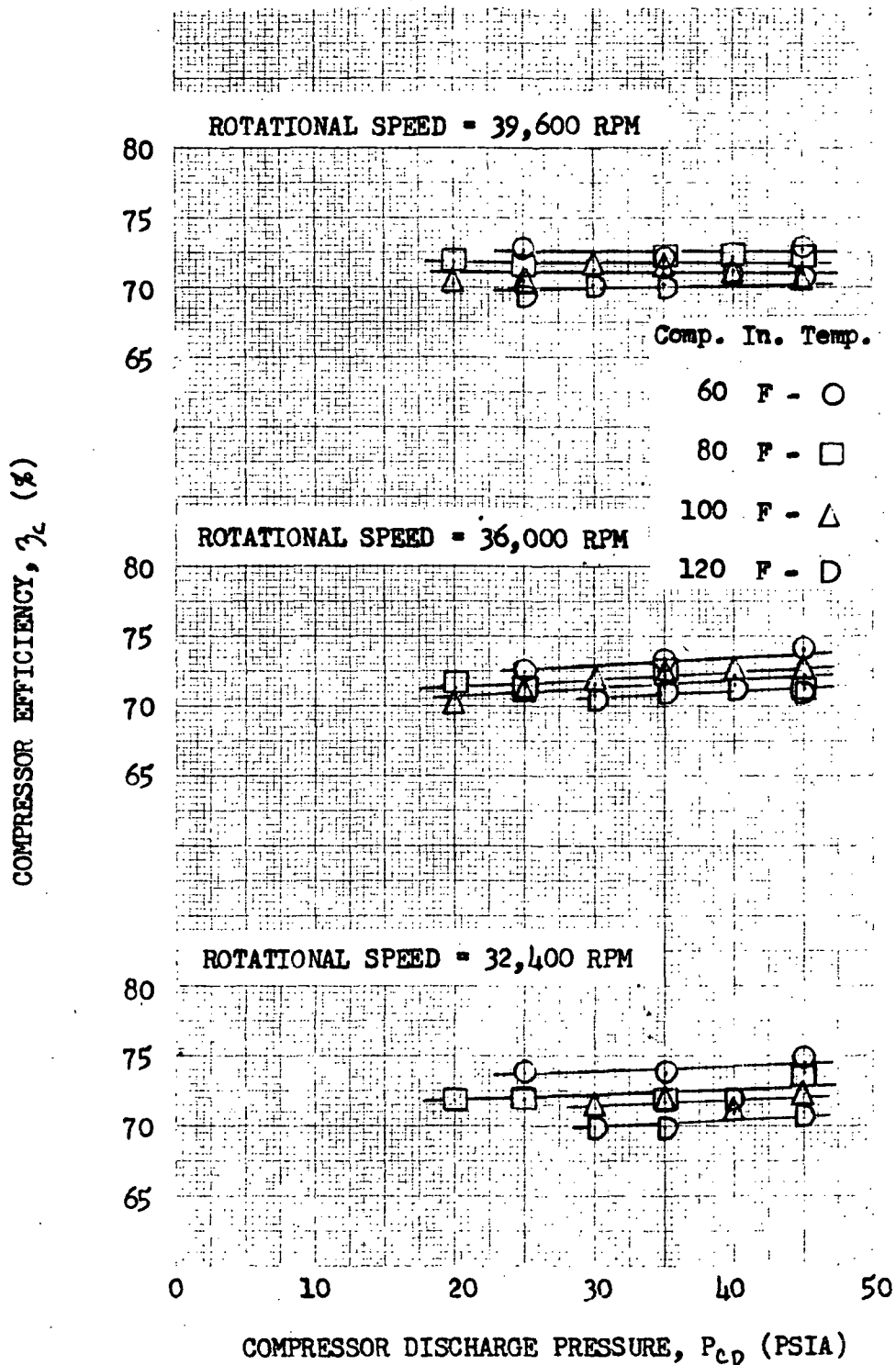


Figure 8: Effect of Compressor Discharge Pressure on Compressor Efficiency at Rotational Speeds of 32,400, 36,000, and 39,600 RPM using Helium-Xenon Gas.

(c) Turbine Inlet Temperature 1400 F

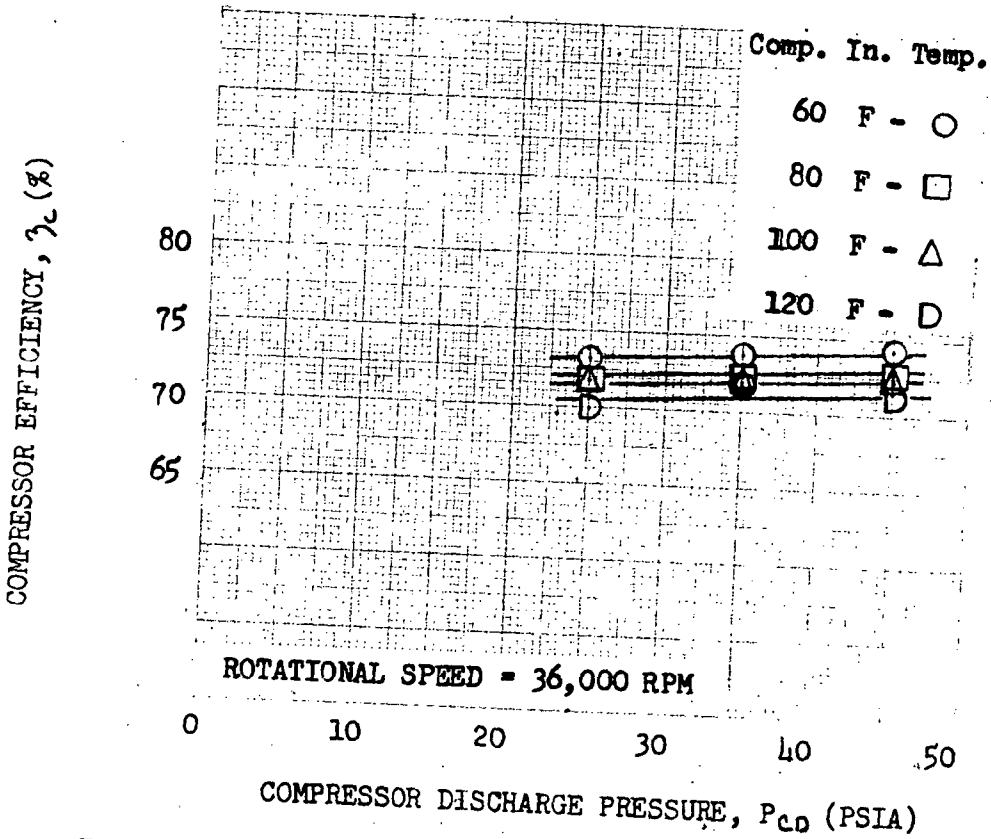


Figure 8: Effect of Compressor Discharge Pressure on Compressor Efficiency at a Rotational Speed of 36,000 RPM using Helium-Xenon Gas.
 (d) Turbine Inlet Temperature 1500 F

COMPRESSOR EFFICIENCY, η_c (%)

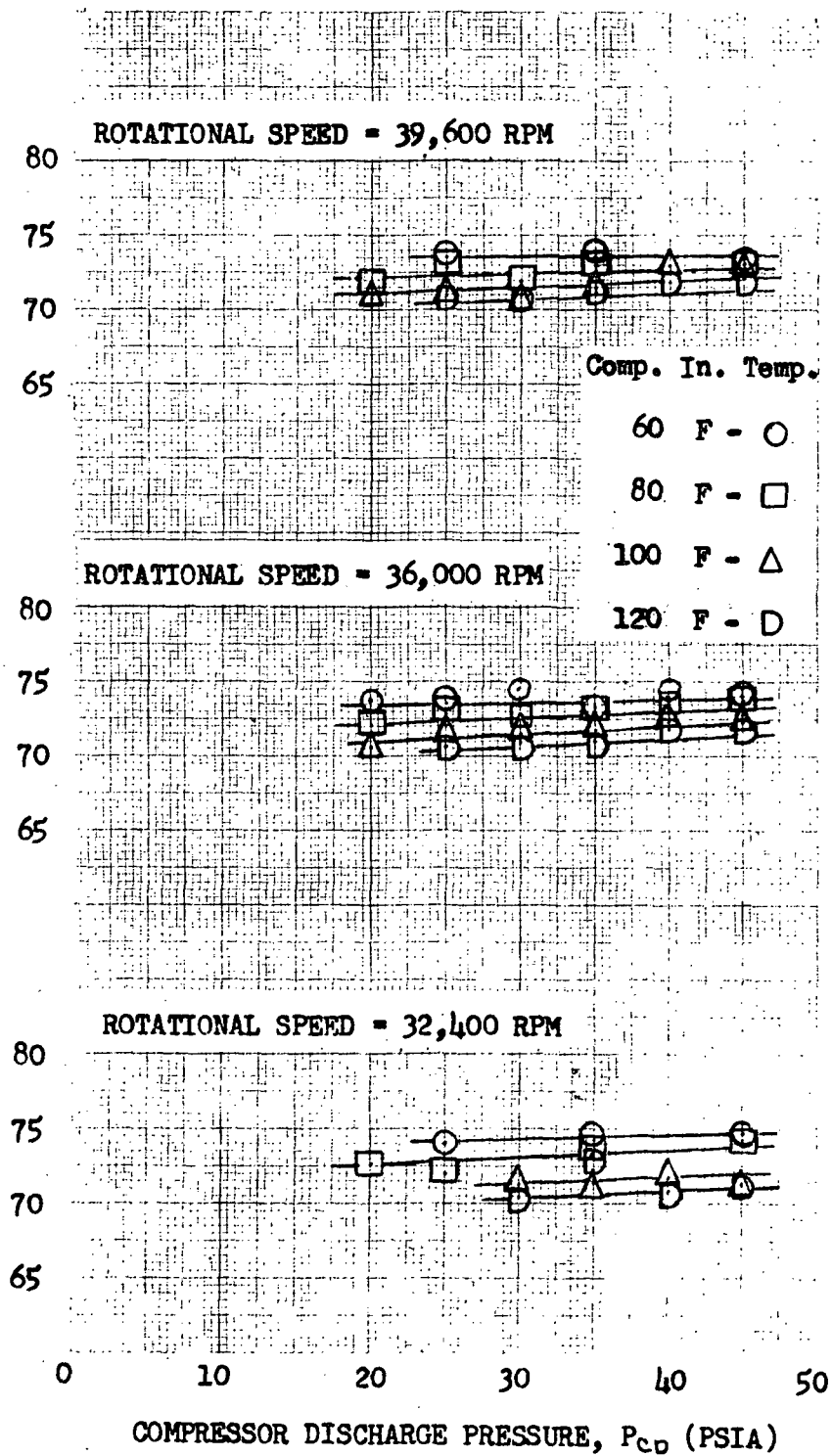


Figure 8: Effect of Compressor Discharge Pressure on Compressor Efficiency at Rotational Speeds of 32,400, 36,000, and 39,600 RPM using Helium-Xenon Gas.
 (e) Turbine Inlet Temperature 1600 F

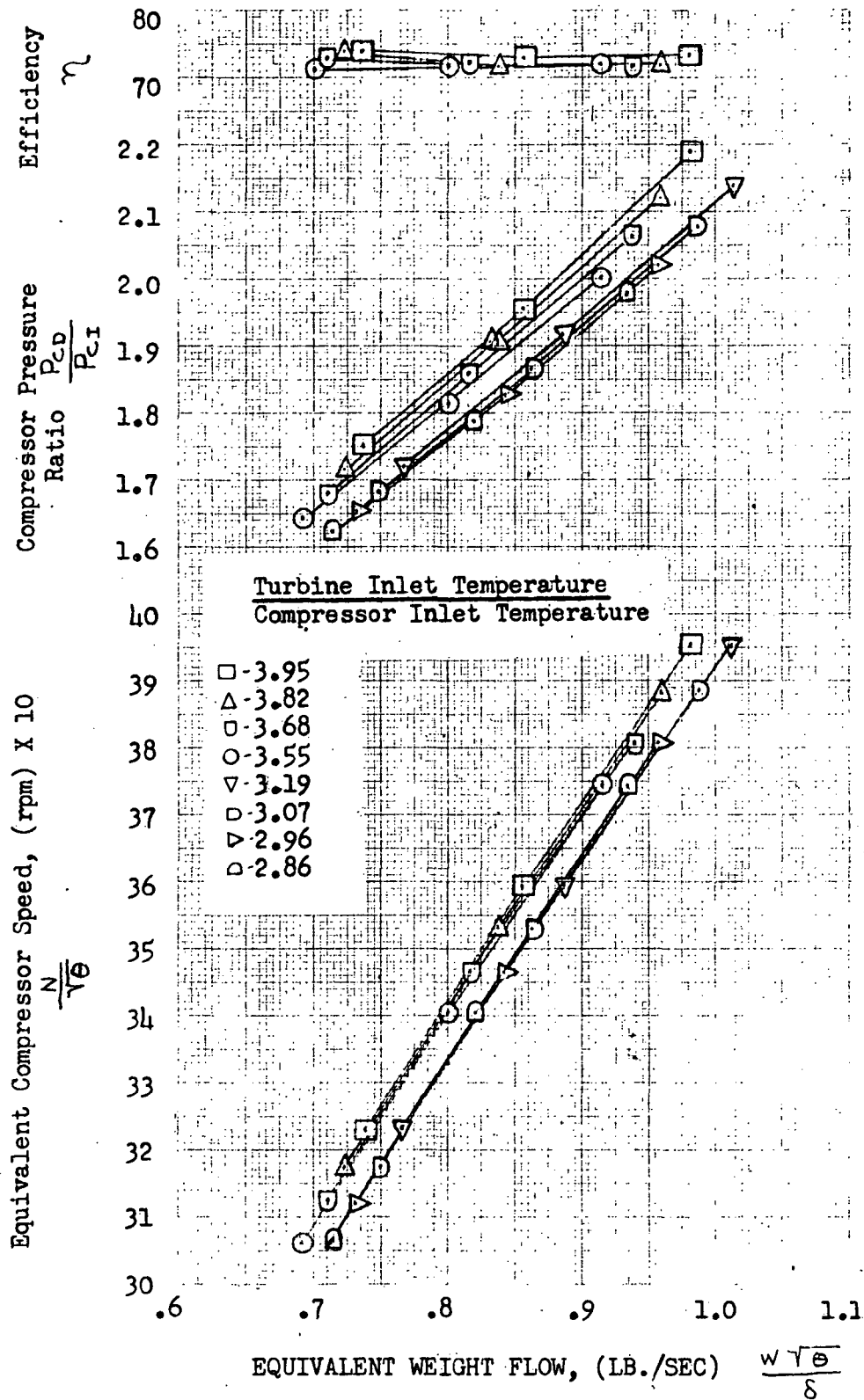


Figure 9: Effect of Equivalent Weight Flow on the Equivalent Compressor Speed, Compressor Pressure Ratio, and Compressor Efficiency.